The DOI for this manuscript is doi: 10.1175/2009JCLI2465.1

The Great 2006 heat wave over California and Nevada: Signal of an Increasing Trend

Alexander Gershunov[1], Daniel R. Cayan[1,2] and Sam F. Iacobellis[1]

[1]Climate, Atmospheric Science and Physical Oceanography (CASPO)

Scripps Institution of Oceanography

La Jolla, CA

[2]United States Geologic Survey

La Jolla, CA

Submitted to the Journal of Climate

Original Submission: February 4, 2008

First Revision: December 7, 2008

Second Revision: June 22, 2009

**Corresponding author address:*

Alexander Gershunov
Climate, Atmospheric Science and Physical Oceanography (CASPO)
Scripps Institution of Oceanography
University of California, San Diego
9500 Gilman Dr. # 0224
La Jolla, CA 92093-0224

Phone: (858) 534-8418; Fax: (858) 534-8561; Email: sasha@ucsd.edu

ABSTRACT

Most of the great California/Nevada heat waves can be classified into primarily daytime or nighttime events depending on whether atmospheric conditions are dry or humid. A rash of nighttime-accentuated events in the last decade was punctuated by an unusually intense case in July 2006, which was the largest heat wave on record (1948–2006). Generally, there is a positive trend in heat wave activity over the entire region that is expressed most strongly and clearly in nighttime rather than daytime temperature extremes. This trend in nighttime heat wave activity has intensified markedly since the 1980s and especially since 2000. The two most recent nighttime heat waves were also strongly expressed in extreme daytime temperatures. Circulations associated with great regional heat waves advect hot air into the region. This air can be dry or moist, depending on whether a moisture source is available, causing heat waves to be expressed preferentially during day or night. A remote moisture source centered within a marine region west of Baja California has been increasing in prominence due to gradual sea surface warming and related increase in atmospheric humidity. Adding to the very strong synoptic dynamics during the 2006 heat wave were a prolonged stream of moisture from this southwestern source and, despite the heightened humidity, an environment in which afternoon convection was suppressed, keeping cloudiness low and daytime temperatures high. The relative contributions of these factors and possible relations to global warming are discussed.

1. Introduction

In July, 2006, California and Nevada were impacted by a heat wave that was unprecedented with respect to the magnitude and duration of high temperatures, especially high nighttime minima, great areal extent, as it simultaneously impacted both Northern and Southern California, and very high humidity levels (Los Angeles Times 2006). This heat wave stressed the delivery of water and energy resources (Davis 2006) and had significant morbidity and mortality impacts on humans and livestock (Knowlton et al. 2009, Munoz 2006, USAgNet 2006). Here, we take a comprehensive retrospective look at the July 2006 heat wave in the context of the region's climate over the past six decades.

Summertime heat waves top the list of stressful weather extremes that are most commonly linked with global anthropogenic climate change (e.g. Easterling et al. 2000a, Meehl and Tebaldi 2004, Tebaldi et al. 2006). Gershunov and Douville (2008) considered the spatial extent of summertime heat over Europe and North America in seasonal average temperature records and model projections, describing the increasing spatial scale of extreme continental summertime heat that is obviously connected to heat-wave activity and clearly tied to global climate change. Heat wave activity has received considerable attention lately, especially following the European heat waves in 2003 (e.g. Beniston and Diaz 2004, Schar 2004, Stott et al. 2004, Meehl and Tebaldi 2004, Gershunov and Douville 2008). Most studies have focused on local extreme temperature magnitudes and durations associated with heat waves (e.g. Beniston 2004, Beniston and Diaz 2004, Schar et al. 2004). However, heat waves are inherently regional phenomena with regional impacts. The spatial scale of heat waves amplifies the event's stressful effects by spreading them over broader sectors of ecosystems, society and infrastructure.

A more precise and useful description of heat wave activity should include an explicit and separate quantification of daily and nightly temperature extremes. During a persistent daytime heat wave, cool nights provide respite from the stressful effects of heat on the health and

general well-being of plants and animals, as well as for the energy sector, and prepare society and nature to face another day of scorching heat. Heat waves strongly manifested at night eliminate this badly needed opportunity for rejuvenation and increase the chances for catastrophic failure in human and natural systems. Extreme daytime heat is known to endanger health most directly via heat stroke but health dangers are exacerbated by associated air pollution including near-surface ozone formation (e.g. Fischer et al. 2004, Stedman 2004, Gosling et al. 2008). Health impacts of nighttime heat are less well known, but there are indications that high minimum temperatures during heat waves enhance morbidity and mortality (Hemon and Jougla 2003, Grize et al. 2005, Gosling et al. 2008). Excess mortality across Switzerland due to the June and August 2003 European heat waves has been attributed to the compounding effect of elevated nighttime temperatures (Grize et al., 2005). During the July 2006 California event, a significant number of victims, most of whom were elderly and living alone, had not used their functioning air conditioning (Margolis et al. 2008). Perhaps they had turned off air conditioning in the evening expecting the strong nighttime cooling characteristic for this region, which did not materialize.

Physical mechanisms causing daytime and nighttime heat waves may differ. Observed warming trends are known to have been stronger at night than during the day (e.g. Easterling et al. 1997, 2000b) resulting in a decreased diurnal temperature range. Stronger nighttime heating trends have been observed at many locations around the globe and, in spite of modeling inconsistencies (Lobell et al. 2007) and recent observations that trends in diurnal temperature range may have ceased globally (IPCC 2007) or may be increasing over some regions (e.g. southern Mexico: Peralta-Hernandez et al. 2008), warmer nights are among the most widespread expectations from anthropogenic global climate change (e.g. Tebaldi et al. 2006). In this regard, the California region has been meeting expectations. The observed summertime average warming here has been largely due to minimum temperatures (not shown). In this topographically, environmentally, economically and climatically complex region, global, regional and local, natural and anthropogenic effects abound (e.g. Duffy et al. 2007; Bonfils et al. 2008).

The purpose of this work is to describe the climatic behavior and regional causes of great heat waves over California and Nevada. Using this foundation, we investigate whether and to what extent the 2006 event may be considered an aberration or a manifestation of a long term change. After describing the data, our approach to quantifying heat waves, and their general behavior (section 2), we illustrate the observed variability of regional daytime and nighttime heat waves (3), describe the synoptic characteristic of the greatest observed events in recent history (4), and explain the 2006 event in that context (5), as well as in the context of trends in daytime and nighttime heat waves (6).

2. Quantifying heat waves

There is no one objective and uniform definition of "heat wave". Heat waves are typically defined locally with specific applications in mind. Mortality increases sharply when extreme heat persists (e.g. Sheridan and Kalkstein 2004). Consequently, health applications tend to stress duration and require that events last at least 2-3 days, but specific details vary regionally. Gosling et al. (2008) provide a useful summary of definitions. For example, in China, heat warnings are issued when maximum temperature is forecast to exceed 35°C on any one day, while in the UK, regionally-varying thresholds of maximum and minimum temperature must be exceeded for two consecutive days and an intervening night. The Netherlands meteorological bureau issues warnings to health services when maximum temperatures are predicted to exceed 25°C for at least 5 days of which at least 3 days threaten temperatures above 30°C. In the United States, the National Weather Service suggests early warning when the daytime heat index (including adjustment for humidity) reaches 40.6°C and a nighttime minimum temperature of 26.7°C persists for at least 48 hours. Various definitions are also adapted in the research literature. For example, Beniston (2004) defines a heat wave when local Tmax exceeds the 90th percentile of local summertime climatology during 3 successive days. Gosling et al. (2007)

require 3 days of excess above the 95th percentile, while Hajat et al. (2002) require that a smoothed 3-day running mean of average temperature exceed the 97th percentile over at least 5 consecutive days. Local duration is obviously important for health applications, while for energy applications, spatial extent and *regional* as opposed to local duration could be more relevant.

In the present study, we seek a straightforward measure that reflects an event's characteristics known to be important in producing regional impacts on environment and society, e.g. health, infrastructure, economy, etc.. The desired measure would be simply computed from the available data. The resulting heat wave indices should include local components that can be aggregated to represent a heat wave's regional *magnitude*, and therefore, reflect and quantify an event's *intensity*, *duration* and *spatial extent*. As we shall see below, regional duration is a quantity partly related to local duration, but worth considering separately.

a. Observational data

In order to describe the spatial extent of heat waves affecting the California region, their duration, and differential symptoms during day and night, we start with day- and night-time temperatures (Tmax and Tmin, respectively) recorded at ninety-five stations distributed more-or-less uniformly over the adjacent states of California and Nevada. All station data were selected from the updated National Climatic Data Center (NCDC) first order and cooperative observer summary of the day dataset, known as DSI-3200 (NCDC, 2003). The original set of 141 stations with daily Tmin and Tmax records going back to at least January 1, 1948 and running through August 2006 was selected for having no more than 15% of missing data at each station per summer. The choice of 1948 as the starting point was a reasonable compromise between record length and spatial completeness. All stations were purged of unnatural outliers. This original set of stations was characterized by a spatial sampling bias towards most populated areas. The 95 core stations were selected from this original set as representative of the region by keeping one best quality station (i.e. station with the least missing data) per *locale* of 30km radius and thereby

removing the urban density bias. Stations with the most complete records are typically found at lower elevations. To retain the effects of mountain climate diversity important in this topographically complex region, the highest elevation station, in addition to the best quality station, was retained wherever the elevation range exceeded 300m per *locale*. The sparsely populated and observed areas of the southeastern California and Nevada deserts are, by necessity, underrepresented and downplayed by subsequent analyses. We computed local linear summertime Tmax and Tmin trends at all stations and visually examined trend maps for spatial outliers. Time series at several stations exhibiting conspicuous trends were examined for obvious discontinuities and outliers possibly exerting undue influence on the linear trends, but none were found. Although no formal homogenization procedure was performed, the use of many stations to characterize a region strongly reduces possible biases arising from occasional spurious local glitches.

The seasonal focus here is on summer, June – August (JJA). The largest events tend to occur around the seasonal temperature maximum in mid-late July. Although intense heat waves do occasionally occur in September, they tend to be localized resulting from rather different regional circulations than the extensive events considered here[1]. Including a longer season would not significantly influence our results, but concentrating on JJA sharpens our focus on the largest events.

b. Quantifying regional summertime heat wave activity

Daytime and nighttime heat-wave activity indices were derived to reflect the overall magnitude of extreme summertime heat consisting of intensity, frequency, duration and spatial extent of daytime and nighttime heat waves. A *local* heat wave is defined to occur when temperature at a particular station (j) exceeds the 99th percentile of its local summertime

[1] The September 1978 daytime heat wave expressed along the south and central coast was one such example that resulted from an intense Santa Ana condition. Santa Ana is uncommon in spring and summer.

climatology computed over the base period 1950 – 1999 (Figure 1) for duration of at least 1, 2 or 3 consecutive days or nights. On dates (d*) when station temperatures exceeded these climatological values, we computed the local temperature excesses ($Tmax^{j,d*} - Tmax^{j,99}$, d* marks date when $Tmax^{j,d} > Tmax^{j,99}$, at station j, on all other dates, the quantity is defined as zero) and summed them over each summer (s), obtaining the *local summertime* Degree Day index, $DD_{99}^{j,s} = \Sigma_d(Tmax^{j,s,d} - Tmax^{99,j})$, for d ranging from June 1 to August 31, the 92 days of summer (d=1,…,92), resulting in an annually resolved time series at each station. Three versions of $DD_{99}^{j,s}[n]$ were computed given specific minimum durations of n = 1, 2 and 3 consecutive days. The local summertime Degree Night index ($DN_{99}^{j,s}$) is similarly defined from Tmin. By definition, $DD_{99}^{j,s}$ and $DN_{99}^{j,s}$ represent the intensity and frequency of intense (the hottest one percent for $DD_{99}^{j,s}[1]$ and $DN_{99}^{j,s}[1]$, and progressively rarer given longer duration) local summer heat waves expressed during the day and night, respectively (Table 1).

Properties of $DD_{99}^{j,s}$ and $DN_{99}^{j,s}$ can be understood by plotting Tmin and Tmax. At Sacramento (Weather Service Office station), the larger variance of summertime daily Tmax compared to that of Tmin is apparent on Figure 1, panels a and b. The distribution of Tmin is skewed, having a sharp lower limit and a more volatile upper bound; the well-defined lower threshold indicates that nighttime lowest values are limited, probably because cooling at night is predominantly radiative and is thus time-limited, while large extremes on the hot side are not bounded by an equivalent physical process. Summer 2006, in late July, featured an extremely intense and persistent heat wave and is used here as an example. July 22-24 Tmin at Sacramento was unprecedented over the historical record, reaching 29°C on July 23. The 99th percentile of 22.8°C was exceeded for seven (six consecutive) nights. Tmax, meanwhile, although not unprecedented, exceeded the 99th percentile (42.2°C) for two straight days (July 23-24) and generally varied more symmetrically around the climatological mean values.

To define *regional* heat wave activity, we first compute the 99th percentiles at all stations (Figure 1c,d). This result indicates that the highest temperature extremes during both day and night typically occur in the southeastern low deserts and interior valley regions, while the lowest hot extremes occur in the high Sierra Nevada and along the coast and coastal ranges. Extremes of both Tmax and Tmin display a very similar spatial distribution with few local exceptions, e.g. the southern California coast exhibits relatively hot extremes at night while the northern coastal hills are relatively more prone to intense daytime heat.

The 99th percentile temperatures are used to quantify regional heat wave activity simply by summing threshold exceedances (departures over these local thresholds) over each summer and all stations given three minimum local durations (Figure 2). These indices, DD_{99}^{s} and DN_{99}^{s}, reflect region-wide summertime heat wave activity, i.e. intensity, frequency, duration, and spatial extent of individual heat waves aggregated over each summer (Figure 2a,b). The significant trend in *daytime* heat wave activity for local durations of at least 3 days (n=3) is mostly due to enhancement towards the end of the record. In contrast, the increasing trend in *nighttime* heat wave activity is a feature of the entire record that holds regardless of local duration, although it is accentuated by the most recent summers 2003 and 2006, each unprecedented (Figure 2b). The broad coherent patterns of entirely positive correlations of regional DD_{99}^{s} and DN_{99}^{s} with local values (a median correlation of 0.50/0.48 for $DD_{99}^{j,s}$/$DN_{99}^{j,s}$ for n=1) indicate the widespread nature of intense heat waves (Figure 2c,d).

The observed trend includes California's major population centers around the Bay area and Southern California, but operates at broader scales involving most of California and Nevada, and likely larger areas. A correlation analysis (Figure 2c,d) demonstrates that the *regional* daytime and nighttime heat wave indices are appropriate measures that capture the summertime heat wave *activity* in California-Nevada.

c. Overview of Definitions

The terminology adapted in this article to describe heat wave ***magnitude*** (M) is summarized in Table 1. *Local* (daily and nightly), *seasonal* and *regional* magnitudes, as well as magnitudes of specific events are described below. *Regional duration* is defined as the number of consecutive days or nights when local thresholds are exceeded. *Spatial extent* is defined as the percentage of representative stations where local thresholds are exceeded. *Peak* seasonal (or event) magnitude and spatial extent are defined as the maximum daily value over a season or over the duration of a particular heat wave as appropriate. Regional duration, as well as spatial extent and magnitude, certainly depend on local duration, but local-scale meteorology complicates this scaling up process to the regional level. We sometimes apply the terms "total" or "overall" to mean aggregated measures over space and/or time. Regional magnitudes are displayed as averages over all stations, i.e. in locally meaningful temperature exceedance (i.e. degree days/nights) units. "Daytime" and "nighttime" events refer to heat wave *types*, not the diurnal character of the data used to describe them, e.g. either type of event has a signature in both Tmax and Tmin.

3. Hot summer days and nights

We next examine the frequency and magnitude (i.e., duration, intensity and spatial extent) of regional heat waves more closely at daily and nightly resolution. Figure 3a documents the magnitude of extreme heat waves of unspecified local duration (n=1) for each day and night on our 59-year record. Figure 3b shows the same information for heat waves of 3 or more days/nights local duration (n=3). Timing and duration of strong heat waves can be visually identified on these plots[2]. Regionally,

- heat waves tend to cluster between late June and mid-August,

[2] Both panels represent regional heat waves, whether locally persistent or not. Panel b may be more relevant to health professionals, while panel a may be of greater relevance to energy providers. We do not display the intermediary figure based on local durations of at least 2 consecutive dates (n=2).

- daytime heat waves occurred sporadically throughout the 59-yr period,
- nighttime heat waves have markedly increased in occurrence since the 1970's,
- heat wave activity in both Tmin and Tmax has increased considerably since 2000,
- the largest Tmax events nearly always have *some* expression in Tmin and visa versa.

These observations hold for regional heat waves, regardless of their minimum local duration. Detailed comparisons between the red and blue bubbles (DD_{99} and DN_{99}) on Figure 3, as well as the intraseasonal temporal correlations between them (Figure 4), suggest a temporal coupling between hot Tmin and Tmax extremes that is strong during active summers and has strengthened since about 2000 as heat wave activity has increased.

While overall summertime magnitude of regional heat wave activity was summarized in Figures 2 and 3, each summer's peak regional heat waves can be summarized, by their maximum intensity (Figure 5a,b), spatial extent (Figure 5c,d) and duration (Figure 5e,f) components.

The regional components of daytime heat waves and their positive trends (Figure 5a,c,e and Table 3) suggest that the weak positive trend, especially in locally persistent daytime heat wave activity (Figure 2a and Table 2), can be attributed mainly to increasing regional duration (Figure 5e), somewhat less to spatial extent (Figure 5c), and least of all to maximum magnitude (Figure 5a). Nighttime heat waves have undergone acceleration toward higher levels of activity in all their regional components.

4. Anatomy of great heat waves

Before considering synoptic characteristics of July 2006 compared to other large events, we describe the timing and canonical features of a handful of the largest daytime and nighttime events on record, which we call the "great" heat waves. Below, only results computed for events of unspecified local duration (n=1) are presented for brevity and because they are largely representative of all regional heat waves.

a) The greatest events: case studies

To illustrate the general appearance of great day- and nighttime heat waves, we identify six of the most extensive and intense daytime and nighttime heat wave episodes on record. Figure 6 presents the timing and magnitude of largest events chosen according to results presented in Figures 2, 3 and 5 and emphasizing the greatest magnitude, events defined without regard to local duration. Statistics for these events, moreover, are presented in Table 4.

With the exception of 2006 and 2003, the greatest daytime heat waves have been larger overall than the greatest nighttime events. Extreme nighttime heat accompanied the great daytime heat waves to some degree and visa versa. Regional durations are generally about a week for most great heat waves, but can persist for 2-3 weeks, e.g. 1961, 2003 and 2006. Each great event has a well-defined peak date or two. As far as spatial extent (Table 4), all six of the great daytime heat waves were of comparable scale, with about 40% of the stations registering extreme Tmax on the peak day. *In contrast, during the great nocturnal heat wave of 2006, 74% of our stations recorded extreme Tmin values on July 23, 2006, an event without recorded parallel on the 59-year record (Table 4)*.

In the first five decades on record, nighttime heat waves were of smaller magnitude than daytime events, but this has lately changed. Nighttime events of 2001, 2003 and 2006 have each set successive magnitude records. Daytime heat wave activity is increasing markedly, not in magnitude but in the fact that the most recent great daytime events were daytime expressions of huge nighttime events, e.g. 2003, 2006. During the day, July 2006 is fourth in terms of daytime peak intensity, but its impressive regional duration makes it first among *daytime* events in terms of overall magnitude.

b) Synoptic aspects of great daytime and nighttime heat waves: a canonical view

Here, we are specifically interested in comparing synoptic characteristics of great daytime and nighttime heat waves and understanding the unprecedented 2006 anomaly. We start by describing synoptic features for the canonical peak date of California heat waves and then examine the temporal evolution of their most salient features with the intent to understand causal relationships. Circulation and precipitable water data are from NCEP/NCAR reanalysis representing 24-hour averages. "Daytime" and "nighttime" refers to heat wave event type, not the diurnal character of the reanalysis data.

Synoptic features of great heat waves can be identified by compositing circulation anomalies at the surface (mean sea level pressure or MSLP and wind at sigma level 995) and the free atmosphere (500mb geopotential height) as well as precipitable water (PRWTR) on the peak day of the five largest daytime and nighttime events (Figure 7). These dates are listed in Table 4. The two largest daytime and nighttime events (July 1972[3] and 2006) are considered separately.

Great heat waves are associated with a baroclinic structure in the atmospheric circulation involving horizontal and vertical motions conducive to hot regional weather (Figure 7a-d). The day and nighttime heat wave surface circulation composites (Figure 7a,b) show an anomalous surface pressure gradient sloping southwestward from the Great Plains to the Pacific Coast causing anomalous surface convergence into California. Regional circulation during the peak day in daytime events is characterized by an anomalous surface High that has moved[4] southward along the Front Range of the Rockies into the central and southern Great Plains, a surface Low

[3] The 1972 heat wave was the largest purely daytime event, but it differed considerably in its circulation from the other great heat waves. The event featured a surface High over British Columbia with a southeastern branch extending into the Great Basin together with a pronounced surface Low over the central California coast, creating a state-wide version of a Santa Ana condition, i.e. strong northeasterly flow from the high deserts down into the low valleys of interior and coastal California. This produced subsidence, drying and adiabatic heating. The upper-level anticyclonic circulation was displaced southwestward of its canonical location and moisture levels were below normal over California. For brevity, these results are not shown, but because this event was, in terms of synoptic circulation, so different from the rest, we exclude it from daytime event composites.

[4] Dynamic cartoons of these maps spanning the evolution of events clearly show this development but cannot be fully reproduced in this static format.

off the California coast and a broad High several degrees longitude west of the Washington coast. During peak daytime events, these features bring convergent surface winds into California particularly from the south (see below). During peak nighttime events, the Great Plains High tends to be stronger and more extensive while the other features, including the California Coastal Low, are weaker (to the point of being insignificant[5] in this case) making for reduced anomalous convergence, especially from the Great Basin, i.e. from the high Nevada desert. The circulation aloft (Figure 7c,d) consists of a broad and intense High centered above Washington State. Slight differences between daytime and nighttime canonical event circulation composites are not significant; they are within the range of variability of each of the two samples of five intense day and nighttime events.

While circulation at the surface as well as aloft appears rather similar for peak dates of both daytime and nighttime events, atmospheric moisture content presents a sharp contrast (Figure 7e,f). Nocturnal events are about twice as moist as climatological normals (PRWTR anomaly twice the normal of about 18 kg/m^2 for JJA averaged over this arid region). For daytime events, the average anomaly is slightly (insignificantly) drier than normal over the California and Nevada box. It is generally (i.e. climatologically) not cloudy and, aside from occasional mountain and desert thunderstorms, does not rain over this arid region in summer. However, available moisture levels during the great heat waves of the humid nocturnal variety may be enough to briefly modify this general picture and depress daytime temperatures. We will examine precipitation and cloudiness in section 5d below. *At this point, however, evidence clearly indicates that the enhanced greenhouse effect of water vapor is what mainly upholds nighttime temperatures during nocturnal heat waves.* Figure 7f shows elevated moisture levels especially in southern California as well as to the south-southwest of the region during regional nocturnal heat waves.

[5] The relevant noise distribution consisted of 1000 5-day composite anomaly maps that were re-sampled (bootstrapped) from the data using the base period (1950-1999). By design, and for realism's sake, the re-sampling scheme selected July dates with twice the probability of either June or August.

5. The July 2006 heat wave compared to other great events

a) *Synoptic characteristics on peak date*

The peak of the 2006 event was characterized by circulation rather similar to other great heat waves, especially those of the daytime variety (compare Figures 8a,b and 7a-d). In this case, the surface Low off the California coast was particularly strongly developed. Strong teleconnections were present upstream and downstream of the regional MSLP anomalies. At the 500mb level, the geopotential height over Washington State was impressive with a positive anomaly of 206 meters. There was enhanced moisture over the entire region, with a significant[6] positive anomaly over Nevada. On July 23 2006, moisture over most of California reached levels that were comparable with other great nocturnal heat waves. While these values are impressive, they are only one component explaining why the July 2006 heat wave was so exceptional in its magnitude. To better understand its causes requires a view of its time evolution rather than just a static snapshot of the peak date.

b) Magnitude evolution of 2006 and other great heat waves

The evolution of the 2006 event regional magnitude compared to the canonical daytime and nighttime events is presented in Figure 9. Notably, daytime (Tmax) expressions of nighttime events typically peak one day prior to the main (i.e. nighttime) peak (blue envelope on Figure 9a), and nighttime peaks associated with primarily daytime events tend to occur just after the main (i.e. daytime) peak at date zero (red envelope on Figure 9b).

The evolution of 2006 daytime (Tmax) expression is fully consistent with the average of the largest daytime heat waves, except that strong anomalous regional heating took place 7-5 days prior to the main event and daytime heat subsided more slowly than expected (Figure 9a). Its

[6] Compared to noise distribution re-sampled as described in footnote 6 but using 1-day random maps.

nighttime expression was unprecedented among all other nighttime events, more intense at the peak and more persistent at unprecedented levels. The sizeable warming that occurred over several nights and days before the onset of the main event was of magnitude and duration comparable to our canonical great nighttime heat waves. This prelude may have played an important role in setting the stage for the main event that peaked on July 23.

c) Synoptic dynamics

Figure 10 displays the evolution of circulation and moisture anomalies during the 2006 heat wave compared to the canonical daytime and nighttime events. We show the temporal evolution of key circulation and moisture indices of day and nighttime heat wave activity, e.g. surface pressure gradient expressed as difference of MSLP anomalies over the central/southern Great Plains and coastal California waters, circulation aloft (Z500 over Washington State, and precipitable water averaged over California and Nevada. Low-level convergence and temperature advection into the California and Nevada box are also displayed on panels d and e. Vertical velocity (omega at 850hPa) averaged over the box is displayed on panel f. Averaging was done in boxes displayed on Figures 7 and 8, while the time frame is identical to that of Figure 9 for convenient comparison: temporal evolution over 31 days centered on the peak date of heat waves.

The salient results of Figure 10 can be summarized as follows. The July 2006 low-level circulation evolution described by the mean sea level pressure gradient across the region (Figure 10a) is not significantly different up to the peak date between daytime and nighttime events. The gradient observed in 2006, although building up unusually early, is not unprecedented. However, the geopotential ridge aloft is unprecedented in its strength and early development preceding the surface pressure gradient anomalies by at least one day (Figure 10b, and cross-correlation functions, not shown). For canonical events, temperature anomalies tend to reach the peak within 2 days of the initial warming (Figure 9), approximately in sync with surface pressure gradient anomalies (Figure 10a), while the upper-level ridge ramps up at least one day earlier (Fig 10b,

and cross-correlation functions, not shown). This earlier development of the ridge aloft, typical of canonical events, suggests that the large-scale circulation aloft precedes and drives surface pressure anomalies as well as advection of heat and humidity, when available, leading to different flavors of regional heat waves.

The separation of precipitable water accumulation into and past the peak dates of great daytime and nighttime heat waves is clearly visible on Figure 10c. The magnitude of moisture accumulation in July 2006 was unprecedented. The buildup of moisture started early, in unison with the circulation anomalies, and continued up to one day past the event's peak suggesting that a strong moisture source was present nearby for advection[7]. Other differences between evolutions of daytime and nighttime events are not nearly as consistent. Low-level convergence (Figure 10d) is similar for day- and night-time heat waves. Warming by advection (Figure 10e), however, tends to start earlier for canonical nighttime compared to daytime events. In both cases, it is mainly from the south with contributions from the east and west (directional detail not shown). On the other hand, daytime events tend to be characterized by anomalous subsidence several days prior to the peak (Figure 10f). The stronger subsidence can create and exacerbate the hot and dry atmospheric conditions leading up to the daytime event peak (Figures 9a and 10c).

In July 2006, heat advection started early and with unprecedented strength, weakening into the main peak and recovering afterwards, prolonging this unprecedented event. We note that delayed convergence of heat and moisture (Figure 10d,c) is typical of day- and night-time events and does not seem to be driven simply by the large-scale circulation anomalies which tend to be on the decline after the peak heat wave date. It may be that regional heat and moisture start driving surface convergence via hot air expansion and convective processes following the peak of nighttime events in particular. If this is the case, it could explain (together with somewhat stronger temperature advection past the peaks of daytime events) why nighttime heat waves cool

[7] In this arid region dominated in the summertime by subtropical high pressure, moisture is advected.

faster than daytime events (Figure 9) and, although this was not the case in 2006, why daytime temperatures tend to be depressed during humid nighttime heat waves.

d) Precipitation, cloudiness and maximum daytime temperatures

Precipitation data are available daily at all 95 stations used in this analysis (NCDC 2003). Figure 11 shows daily accumulations of area-averaged precipitation following convention established in Figures 9 and 10. Although precipitation is a noisy variable, we can plainly see that *all* nighttime heat wave peaks are followed by significant precipitation for four days after the peak date with *median* rainfall up to 1mm per station on day 3. While this may not seem like much rain, it is a significant amount for this arid predominantly Mediterranean climate region during the dry season. In July, it rains on average 1.2 days a *median* of 1.5mm per rainy day for a monthly total of 4.8mm (3.8mm) per mean (median) station. June and August are somewhat rainier (9.8 and 6.9 mm monthly total per mean station, respectively), so that in an average summer month, there are 1.6 rainy days (including trace amounts), it rains a median of 2mm per rainy day, a mean (median) monthly total of 7.1 (6.1) mm per station. Any amount of precipitation is highly unusual at a vast majority of stations on any summer day, especially in July. There has been recorded rain over the region on each of the several days of and following the peaks of each of the great nighttime heat waves on our record (Figure 11). The rainfall amount accumulated over the one week period from day -1 to day 5 surrounding the peak date (day 0) of a canonical (i.e. average of five) nighttime heat wave amounted to exactly the average monthly total for the month of July (4.8mm per station). During nighttime heat waves, it obviously doesn't rain at all stations but rainy stations may experience downpours. Besides local soil moisture effects, the associated cloudiness may be widespread enough to strongly depress maximum temperatures via increased albedo. The great humid event of 2006, however, was, in terms of rainfall, in line with seasonal climatology and close to dry daytime events, suggesting a

radiative explanation, involving reduced cloud cover and albedo, for the unusually large Tmax magnitude of this predominantly nighttime event (see below).

Figure 12 presents the Tmax expression of four heat waves: 2006, 2003, 2002 and 2001. Obviously, the Tmin expressions of 2006, 2003 and 2001 are more substantial, but we do not show them here. Superimposed on temperature exceedances accumulated over the duration of each event ($DD^*_{99}{}^j$), we show local precipitation accumulation over exactly one week starting 1 day prior to peak date and ending 5 days after the peak. During this week, cloudiness and soil moisture should be important in suppressing daytime maximum temperatures associated with the peak and its eventual decline. We note that the great 2006 event, in spite of its unprecedented precipitable water accumulation, was characterized by low precipitation amounts at few stations compared to the other nighttime events, specifically the two recent ones: 2003 and 2001 (Figure 12: compare panel a to panels b and d). Precipitation accumulated over the region during the 2003 event was below the nighttime event median. The 2001 event was typical of great nighttime heat waves: it was very wet in terms of both spatial extent and precipitation amount which must have strongly reduced its temperature expression during the day. The 2002 event was typical of dry daytime heat waves: it featured low precipitation amounts and that only over a few mountain and desert stations. The great 2006 event with 26% of stations recording precipitation with average weekly accumulations of 3.4mm/station was only slightly wetter than 2002. Specifically, precipitation did not materialize over the Central Valley where temperatures and humidity were at record-breaking levels at most stations.

Geostationary satellite imagery[8] covers the four events displayed in Figure 12. Figure 13 shows albedo averaged over California and Nevada from 8 days before to 8 days after peak dates

[8] Albedo data was obtained from GOES-10 (2000-2003 events) and GOES-11 (2006 event) satellite imager visible channel measurements. Horizontal resolution of the albedo measurements is approximately 1 km. Post launch sensor calibrations were performed using the algorithm of Nguyen et al. (2004) (also available at http://angler.larc.nasa.gov/cgi bin/site/showdoc?mnemonic=SAT_CALIB_USER) Visible channel pixels over the land regions of California and Nevada were used to compute average albedo values.

of the 2006, 2003, 2002 and 2001 events. These composites are displayed for 10, 12, 14 and 16 hours local time. The spatial cloud patterns (not shown) are consistent with station rainfall. The wet 2001 event (Figure 13d) shows a strong peak in regional albedo for days -1 to 3 around peak date with a maximum of almost 50% at 16 hours on day 2 after peak date. Strong diurnal enhancement of albedo with a late afternoon peak on cloudy days is clearly characteristic of convection. Convective cloudiness was also present during other events, but it was progressively more spatially limited in 2003, 2006 and 2002. In mid-July 2006, convective clouds and precipitation reduced the daytime expression of the "prelude" to the main event on days -3 and -4, but then abated allowing maximum temperatures to rise sharply into the main peak (Figure 9). Specifically, the peak day did not generally see convective cloudiness in 2006 (albedo did not peak at 16 hours) allowing record breaking daytime temperatures, while the high humidity prevented nighttime cooling. The persistent 2003 event was most strongly expressed over the mountains and deserts. Its peak was almost as convective as that in 2001, but was then followed by a lull in convection.

The 2002 and 2001 events were typical of dry daytime and humid nighttime heat waves, respectively, in terms of atmospheric humidity (i.e. precipitable water) and precipitation. Although satellite data are not long enough to verify this directly, the link with precipitation allows us to infer that these events were also typical of their type in terms of cloudiness. The 2006 and, to a lesser extent, 2003 events were atypical – there was plenty of atmospheric humidity to make them predominantly nighttime events, however, widespread cloudiness and precipitation did not materialize, allowing daytime temperatures to rise to levels typically associated with the greatest daytime heat waves.

The reasons for this weak convection observed during the most recent two great heat waves (especially 2006) in the presence of so much heat and moisture are beyond the scope of this article. On the one hand, it is surprising to see so much convection depressing daytime temperatures during "typical" great nighttime heat waves in this normally arid Mediterranean

climate. On the other, convective suppression during such events is even more surprising and could be detrimental were it to re-occur during future humid heat waves.

6. Trends

From the above account, it is clear that the causes of heat waves over California and Nevada are complex and that numerous conditions coincided to create the unprecedented heat of July 2006. One of these conditions is the observed trend in the probability of more intense, larger, and more persistent nighttime heat waves (Tables 2 and 3). As the 2006 and 2003 events suggest, humid heat waves with suppressed convective cloudiness can result in intense daytime heat associated with primarily nighttime events. This, together with the positive trend observed in the coupling between Tmax and Tmin expressions of heat waves (Figure 5), may account for part of the trend observed in daytime heat wave activity as well. In any case, the strongest trend and the best possibility for its physical explanation are associated with primarily nighttime events. In the final part of this work, we will try to shed some light on this matter by focusing on long-term changes in heat wave activity over this region.

The yet incomplete final decade on our record (1998 – 2006) has already produced much stronger heat wave activity than any of the previous five decades, expressed in both minimum and maximum temperatures. For nocturnal heat waves especially, the trend towards greater heat wave activity is apparent as an orderly progression from one decade to the next (result not shown). The increasing relative magnitude of nighttime versus daytime heat waves is also apparent. This raises the obvious question: Is humidity increasing over the region? Our results, based on the available summertime average precipitable water from Reanalysis (Figure 14a) and sparse *in situ* dew point and radiosonde records (not shown) are not characterized by coherent or significant regional trends over California and Nevada. There is a possibility that the relevant regional humidity changes are episodic, e.g. triggered by the synoptic nature of the heat wave circulations and

therefore not clearly manifested except during heat waves. But what mechanism could possibly account for such a trend?

Although we cannot see a moistening over California and Nevada, Figure 14 (a,b) shows a strong and significant moistening trend centered over the marine region west of Baja California, and more generally to the west-south-west of California State. This is a region where a strong positive trend in summertime sea surface temperature (SST) is observed (e.g. Pierce et al. 2006, their Figure 20). This trend makes anomalous moisture more readily available for California heat wave circulations to advect and more frequently and preferentially intensify the nocturnal expression of California heat waves. Great nocturnal heat waves are characterized by enhanced moisture availability off-shore and to the south prior to the event's development and through its peak, while daytime events are typically preceded by a dry anomaly there (Figure 14c). Heat wave circulations advect air northeastward from this region into California (Figure 14d). The anomalous advection via the southwestern and southern borders of our focus region does not typically take place until the peak date of both daytime and nighttime events. Different humid events must tap different available moisture sources (associated with the southwest monsoon, for example). In 2006, however, advection from the southwestern marine region started strongly five days before the peak and continued for the entire duration of the event. This south-westerly advection was unprecedented; it strongly contributed to the build-up of moisture over the region (Figure 10c and 14d) and preconditioned that great heat wave to be expressed most strongly at night. This coincidence of the moisture anomaly with southwesterly advection was clearly a rare event, but it is made more likely by the strong moistening trend present in this marine source region. Other peaks in the summer PRWTR time series there (Figure 14b) can be identified to correspond to summers with large nocturnal heat waves, e.g. 1990, 1992, etc. The correlation coefficient between this trend (Figure 14b) and overall nighttime regional heat wave activity, DN_{99}^{S}, is 0.48 (Figure 2b), 0.52 with maximal spatial extent (Figure 5d), 0.44 with maximum

regional duration (Figure 5f), and 0.52 with maximum one-day magnitude (Figure 5b), all highly significant.

The regional moistening by advection observed during nighttime heat waves does not occur frequently enough to make for clearly detectable summertime moisture trends over California and Nevada, but its episodic effect on Tmin extremes may be strong enough to be partially reflected in average summertime Tmin over the region.

7. Summary, discussion and conclusions

We have quantified heat wave activity over California and Nevada during summers 1948 – 2006 in terms of regional magnitude (relative to local intensity and duration thresholds) and its components: intensity, spatial extent and duration. Heat waves typically impose a regional footprint and can be classified into primarily dry *daytime* and humid *nighttime* events, those with the greatest regional magnitudes expressed in Tmax or Tmin, respectively. Daytime (nighttime) events typically have sizeable but far smaller expressions in Tmin (Tmax).

The atmospheric circulation anomalies responsible for most great daytime- and nighttime-type California heat waves are remarkably similar consisting of a prominent anticyclone aloft above Washington State. This feature reinforces a strong surface pressure gradient between a high pressure anomaly over the Great Plains and a Low off the California coast. This synoptic pattern produces low-level heat advection into California and Nevada. The main feature that distinguishes nighttime from daytime heat waves is the anomalously moist atmosphere during nighttime events. The moisture advected over California and Nevada can reach twice its normal levels and help maintain exceptionally high nighttime temperatures via the elevated greenhouse effect of a moist atmosphere. Elevated moisture and temperature also typically result in convective cloudiness and precipitation that depress daytime maximum temperatures. This tends to limit nighttime temperatures and keep anomalous Tmin and Tmax

magnitudes lower during most nighttime heat waves compared to the Tmax magnitudes of dry daytime events. Dry daytime heat waves are characterized by soaring Tmax, while radiative cooling efficiently reduces Tmin. Thus, the presence of humidity during heat waves normally suppresses daytime temperatures, but its absence diminishes nighttime temperatures, both via radiative effects. The expected positive feedback between Tmin and Tmax, therefore, may be weakend during either type of California heat waves.

This general picture has been changing, however. Regional magnitudes, as well as their components (intensity, spatial extent and duration) are increasing, particularly for humid nocturnal heat waves, which have tended to cluster and amplify towards the end of the record. These changes in regional heat wave activity are related in part to the presence of an increasing Pacific moisture source to the southwest of California State, west of Baja California. The coupling between daytime and nighttime temperature expressions of heat waves has also been strengthening significantly throughout the 59-year record. The most recent great heat waves on record, namely 2003[9] and 2006, were primarily nighttime events. These events lasted over two weeks each and far exceeded previous highest nighttime magnitudes. Furthermore, they have had overall daytime expressions to match or exceed, in the case of 2006, the greatest observed daytime heat waves.

In mid-July 2006, beginning early (July 15-20)[10] in advance of the peak of the great heat wave that occurred on July 23, the large scale upper-level circulation pattern and regional humidity anomalies over California and Nevada were remarkably strong, Humidity, which exceeded previous heat waves, was advected particularly from the southwest. Strong and persistent baroclinic circulation resulting in steady low-level convergence kept pumping moisture and heat into the region until unprecedented levels of more than twice the normal summertime

[9] July10 – August 2, 2003, was the most intense and extensive nighttime event up to that time, 3 times greater in overall magnitude than the previous record (2001). It was characterized by relatively low convection and a strong daytime expression, placing it third on the list of *daytime* events.
[10] July 19th, 2006, saw the 7th greatest one-night spatial extent of extreme heat on the 59-summer record.

atmospheric precipitable water collected over California and Nevada. For reasons not yet understood, convection was suppressed and the overall daytime temperature expression of the 2006 event surpassed all *daytime* heat waves on record. This conspicuous relative absence of convection in the presence of so much moisture led to intense daytime warming which in turn promoted more intense and extensive nighttime heat, without any observed precedent. The positive feedback between Tmax and Tmin strengthened and made the heat wave more intense, widespread and persistent.

Mechanisms that support the positive feedback between high nighttime and high daytime temperatures seem particularly crucial to understand, in view of the dangerous effects on human health and other biological impacts. Although controls on convective cloudiness and rainfall in the presence of heat and moisture are beyond the scope of this paper, it is noteworthy that (a) aerosol production does, in a complex way, depend on humidity and temperature (e.g. Jamriska et al. 2008), and (b) aerosols can have multiple effects on cloudiness and precipitation (e.g. Ramanathan et al. 2001, Givati and Rosenfeld 2004, Rosenfeld and Givati 2006). Convection, rare for this Mediterranean climate in summer has not, to our knowledge, been studied with respect to aerosol effects. It is possible, however, that elevated summertime heat and moisture, especially under convergent surface wind conditions, may promote higher concentrations of aerosol pollutants that could have multiple effects on clouds and precipitation affecting daytime temperatures. Aerosols might, for example, hamper convection by altering the vertical tropospheric temperature structure. Aerosols are known to impact health risks associated with heat exposure (e.g. Fischer et al. 2004, Stedman 2004, Gosling et al. 2008) and further study is warranted to determine their net direct and indirect effects on maximum temperatures during humid heat wave conditions.

Is the climb in nocturnal heat wave activity that we are witnessing now over California and Nevada simply a regional process? Evidently not. The unusual magnitudes of the most recent California heat waves seem to be partially rooted in the long-term trend of nighttime heat

wave activity and Tmax/Tmin coupling. This trend is related to the availability of an anomalous and increasing moisture source west of Baja California. This moisture source is coincident with a warming SST trend, which appears to be part of the global ocean warming pattern known to be due to anthropogenic climate change (Barnett et al., 2001, 2005, Pierce et al. 2006). To elucidate this process will require an augmented set of tools including dynamical models and their detailed synoptic-level verification. For now we simply note that the recent upturn in California-Nevada heatwaves appears consistent with the regional symptoms of global warming. This suggests a plausible scenario for future summertime heat wave activity in California: more frequent, hotter, more extensive and more persistent humid nighttime heat waves with a growing daytime signature.

Thus, it seems that heat waves should be investigated in a much larger geo-spatial context. Although most severely impacting California, the July 2006 heat wave extended across the conterminous United States as well as into adjacent parts of Canada and Mexico. At the same time, a heat wave also affected most of Europe, although it was not as severe as the great European heat wave of summer 2003. So, while heat waves in California may be unique in their regional causes and details, their observed changes may be largely emblematic in terms of heat wave activity globally. Global climate warming is becoming and is expected to increasingly become more apparent in the mounting spatial scale of regional summertime heat (Gershunov and Douville 2008). Together with our more focused regional results, this further suggests a direct and increasing link between regional heat waves and global climate change.

Acknowledgments

Thanks are due to Mary Tyree and Emelia Bainto for data handling and processing. This work was funded by the California Energy Commission through the California Climate Change Center and by NOAA via the RISA program through the California Applications Center and grant NA17RJ1231-72. This work also contributes to research under NSF grant ATM-0236898, NATO Science for Peace project (SFP 981044), and UC MEXUS-CONACYT project (CN-05-223). Thanks are due to Tereza Cavazos, Hugo Hidalgo, Pasha Groisman, Helene Margolis and Odelle Hadley for useful discussions and to four anonymous reviewers for detailed comments on the original version of the manuscript.

References

Barnett, T.P., D.W. Pierce and R. Schnur, 2001: Detection of anthropogenic climate change in the world's oceans. *Science*, **292**, 270-274.

Barnett, T.P., D.W. Pierce, K.M. AchtaRao, P.J. Gleckler, B.D. Santer, J.M. Gregory and W.M. Washington, 2005: Penetration of human-induced warming into the world's oceans. *Science*, **309**, 284-287.

Beniston, M., 2004: The 2003 heat wave in Europe: A shape of things to come? An analysis based on Swiss climatological data and model simulations. *Geophys. Res. Lett.,* **31,** L02202, doi:10.1029/2003GL018857.

Beniston, M. and H.F. Diaz, 2004: The 2003 heat wave as an example of summers in a greenhouse climate? Observations and climate model simulations for Basel, Switzerland. *Global and Planetary Change*, **44**, 73-81.

Bonfils C., B.D. Santer, D.W. Pierce, H.G. Hidalgo, G. Bala, T. Das, T.P. Barnett, D.R. Cayan, C. Doutriaux, A.W. Wood, A. Mirin, T. Nozawa, 2008: Detection and Attribution of temperature changes in the mountainous western United States. *J. Climate*, in press.

Davis, A., 2006: Heat claims as many as 38 people, tests state energy supply. Associated Press, appearing in San Jose Mercury News, July 25.

Duffy, P.B., C. Bonfils and D. Lobell, 2007: Interpreting recent temperature trends in California. *Eos*, **88**, 409-410.

Easterling, D. R., and Coauthors, 1997: Maximum and minimum temperature trends for the globe. *Science*, **277,** 364–367.

Easterling, D.R., G.A. Meehl, C. Parmesan, S.A. Changnon, T.R. Karl and L.O.Mearns, 2000a: Climate extremes: Observations, modeling, and impacts. *Science*, **289**, 2068-2074.

Easterling, D.R., J.L. Evans, P.Ya. Groisman, T.R. Karl, K.E. Kunkel and P. Ambenje, 2000b: Observed variability and trends in extreme climate events: A brief review. *Bull. Am. Meteorol. Soc*., **81**, 417-425.

Fischer, P., B. Brunekreef and E. Lebret, 2004: Air pollution related deaths during the 2003 heat wave in the Netherlands. *Atmospheric Environment*. **38**, 1083-1085.

Gershunov A. and H. Douville, 2008: Extensive summer hot and cold extremes under current and possible future climatic conditions: Europe and North America. In: H. F. Diaz and R. J. Murnane (Eds.), *Climate Extremes and Society.* Cambridge University Press, New York, 348pp, 74-98.

Givati A., and D. Rosenfeld, 2004: Quantifying precipitation suppression due to air pollution. *J. Appl. Meteorol.*, **43**, 1038-1056.

Gosling, S.N., G.R. McGregor, A. Páldy (2007) Climate change and heat-related mortality in six cities, part 1: model construction and validation. *Int. J. Biometeorol*. **51**, 525-540.

Gosling, S.N., J.A. Lowe, G.R. McGregor, M. Pelling and B.D. Malamud, 2008: Associations between elevated atmospheric temperature and human mortality: A critical review of the literature. *Clim. Change*, DOI 10.1007/s10584-008-9441-x.

Grize, L., A. Huss, O. Thommen, C. Schindler and C. Braun-Fahrländer, 2005: Heat wave 2003 and mortality in Switzerland. *Swiss Med Wkly*, **135**, 200-205.

Hajat, S., R.S. Kovats, R.W. Atkinson, A. Haines, 2002: Impact of hot temperatures on death in London: a time series approach. *J. Epidemiol. Community Health* **56**, 367–372.

Hemon, D. and E. Jougla, 2003: Estimation de la surmortalité et principales caracteristiques epidemiologiques. Paris: ISERM 25 septembre 2003.

Intergovernmental Panel on Climate Change (IPCC), 2007: Observations: Surface and atmospheric climate change. *Working Group 1 Report "The Physical Science Basis"*, Chapter 3, Available at http://www.ipcc.ch/.

Jamriska, M., L. Morawska and K. Mergersen, 2008: The effect of temperature and humidity on size segregated traffic exhaust particle emissions. *Atmos. Environment*, **42**, 2369-2382.

Kistler, R., E. Kalnay, W. Collins, et al., 2001: The NCEP-NCAR 50-year reanalysis: Monthly means CD-ROM and documentation. *Bull. Amer. Meteor. Soc*., **82** (2), 247-267.

Knowlton, K., M. Rotkin-Ellman, G. King, H.G. Margolis, D. Smith, G. Solomon, R. Trent and P. English, 2009: The 2006 California heat wave: Impacts on hospitalizations and emergency department visits. Env. Health Persp., 117, 61-67.

Lobell, D., C. Bonfils and P.B. Duffy, 2007: Climate change uncertainty for daily minimum and maximum temperatures: A model intercomparison. *Geophys. Res. Lett*., **34**, L05715, doi:10.1029/2006GL028726.

Los Angeles Times, 2006: High nighttime temperatures set records too. July 25.

Margolis H.G., A. Gershunov, T. Kim, P. English, R. Trent, 2008: 2006 California Heat Wave High Death Toll: Insights Gained From Coroner's Reports and Meteorological Characteristics of Event. *Conference of International Society of Environmental Epidemiologists*, Pasadena, CA (Presented October 15, 2008; Abstract ISEE-1672, November 2008 Supplement to Epidemiology 19(6): S363-364.)

Meehl, G.A. and C. Tebaldi, 2004: More intense, more frequent, and longer lasting heat waves in the 21st century. *Science*, **305**, 994-997.

Munoz, O., 2006: 139 deaths later, heat wave appears over. *Associated Press*, appearing in Forbes, July 28.

NCDC, 2003: Data documentation for data set 3200 (DSI-3200): Surface land daily cooperative summary of the day. National Climatic Data Center, Asheville, NC, 36 pp. [Available online at http://www.ncdc.noaa.gov/pub/data/documentlibrary/tddoc/td3200.pdf].

Nguyen, L., D.R. Doelling, P. Minnis, and J.K. Ayers, 2004: Rapid Technique to cross-calibrate satellite imager with visible channels. *Proc. 49th SPIE Meeting*, Denver, CO, Aug. 2-6.

Peralta-Hernandez, A.R., R.C. Bowling and L.R. Barba-Martinez, 2008: Analysis of near-surface diurnal temperature variations and trends in southern Mexico. *Int. J. of Climatology*, doi: 10.1002/joc.1715.

Pierce, D.W., T.P. Barnett, K.M. AchtaRao, P.J. Gleckler, J.M. Gregory, W.M. Washington, 2006: Anthropogenic warming of the oceans: observations and model results. *J.Clim*. **19**, 1873-1900.

Ramanathan, V., P.J. Crutzen, J.T. Kiehl, D.Rosenfeld, 2001: Aerosols, Climate, and the Hydrological Cycle. *Science*, **294**, 2119-2124

Rosenfeld, D. and A. Givati, 2006: Evidence of orographic precipitation suppression by air pollution–induced aerosols in the Western United States. *J. Appl. Meteorol. and Climatol*. **45**, 893-911.

Schar, C., P.L. Vidale , D. Luthi, C. Frei, C. Haberli, M.A. Liniger and C. Appenzeller, 2004: The role of increasing temperature variability in European summer heatwaves. *Nature,* **427**, 332-336.

Sheridan, S.C., L.S. Kalkstein, 2004: Progress in heat watch-warning system technology. *Bull. Am. Meteorol. Soc.* **85**,1931–1941.

Stedman, J., 2004: The predicted number of air pollution related deaths in the UK during the August 2003 heat wave. *Atmospheric Environment*, **38**, 1087-1090.

Stott, P.A., D.A. Stone and M.R. Allen, 2004: Human contribution to the European heatwave of 2003. *Nature*, **432**, 610-613.

Tebaldi, C., K. Hayhoe, J.M. Arblaster and G.A. Meehl, 2006: Going to the extremes: An intercomparison of model-simulated historical and future changes in extreme events. *Clim. Change*, **79**, 185-211.

Tukey, J.W., 1977: Exploratory Data Analysis. Reading, Massachusetts: Addison-Wesley.

USAgNet, 2006: California's cattle death toll surpasses 25,000. July 31.

FIGURE CAPTIONS

Figure 1. Observed Tmax (a) and Tmin (b) plotted in dots for every date of every summer on record with average (black circles) and 2006 observations (colored circles) for Sacramento (WSO City station). The 99th percentile threshold (dashed line) was computed over the 1950 – 1999 climatology. By definition, daytime or nighttime heat waves occur on days when Tmin or Tmax exceed this threshold over a given minimum duration (n=1,2,3). They are quantified locally as sums of exceedances over the 99th percentile. Panels (c) and (d) depict the approximate (in bins) 99th percentiles of summertime Tmax and Tmin, respectively, at each station. Regional heat waves are quantified as exceedances over the local 99th percentile, *and given a specific minimum duration,* summed over all stations. "X" marks Sacramento.

Figure 2. Regional seasonal magnitudes, DD_{99}^{s}[1,2,3] (a) and nights, DN_{99}^{s}[1,2,3] (b) as defined in Table 1. Linear regression lines are shown for the entire record (1948-2006) and over the base period (1950-1999, inset) only where slope is significantly different from zero (two-tailed test) at above the 95% significance level (see Table 2). DD_{99}^{s} and DN_{99}^{s} are correlated at 0.6, 0.54 and 0.47, for local durations of at least n = 1, 2 and 3 consecutive days and nights, respectively. DD_{99}^{s} (DN_{99}^{s}) time series are obviously highly correlated with each other, e.g. above 0.99 and above 0.94 for daytime and nighttime events, respectively, given any combination of local durations. The spatial expressions of the region-wide indices (DD_{99}^{s} and DN_{99}^{s}) given local minimum durations of one day or night (n=1) are shown as correlations with local $DD_{99}^{j,s}$ (c) and $DN_{99}^{j,s}$ (d). Correlations greater than 0.22 are significant with 95% confidence. All colored circles represent significant correlations.

Figure 3. The daily-level magnitude of regional heat wave activity as defined in Table 1: $DD_{99}^{s,d}$ (red ovals) and $DN_{99}^{s,d}$ (blue ovals). The x-axis corresponds to each year on record, while the y-axis corresponds to each summer date. Regional magnitude for unspecified local duration, n=1 (a) and local duration of at least 3 consecutive dates (b). The larger the oval, the greater the magnitude. The scale is given by the maximum magnitude recorded each summer and shown at the top of each plot and again in Figure 5a,b. The overall magnitude for each summer is shown in Figure 2a,b.

Figure 4. Correlations between each summer's daily and nightly heat wave magnitude (columns of red and blue bubbles on Figure 3a). This reflects the degree to which regional daytime and nighttime heat waves are coincident, regardless of local duration (n=1). Correlations above 0.17 (0.24) are significant at 95% (99%). Linear trends for the entire period as well as for the base period (1950 – 1999, inset) are statistically significant with over 99% confidence (two-tailed test).

Figure 5. Seasonal maxima of regional heat wave components: total magnitude on the peak day (a) and night (b) of the greatest events, maximum spatial extent in % of stations by day (c) and night (d); and maximum continuous regional duration of daytime (e) and nighttime (f) heat waves. All variables were computed for each summer on record from data presented in Figure 3. Components were computed given local durations of at least 1, 2 and 3 consecutive days/nights (n=1,2,3) and delineated in progressively darker shades of gray. Correlations between these indices and trends are given in Table 3.

Figure 6. Overall magnitude [cumulative temperature departures (°C) in excess of 99th percentile of each station] of the six daytime (gray) and nighttime (black) great heat waves in California region. Thick (thin) lines delineate the heat wave's primary (secondary) expression, i.e. daytime or nighttime. Magnitude is in degree days/nights per average station, i.e. $DD^*_{99} = \Sigma_{j,s^*,d^*}(DD_{99}{}^{j,s,d})$, where s* refers to the particular summer and d* refers to dates spanned by the event.

Figure 7. Surface circulation (wind at sigma level 995, arrows in m/s) and mean sea level pressure in millibars (a,b), 500mb geopotential height in meters (c,d), and precipitable water kg/m^2 (e,f) anomalies with respect to JJA mean. Anomalies are composited for the peak days of the largest five daytime events (a,c,e) and the largest five nighttime events (b,d,f) excluding 2006 and 1972 (see Table 4 for exact dates). The data are from the NCEP/NCAR Reanalysis I (Kistler et al. 2001). Black rectangles outline regions used for evolution plots presented in Figure 10. Contours and colors represent the same anomalies, but only values statistically significant with 95% confidence (two-tailed test) determined via bootstrap re-sampling (performed with 1000 re-sampled 5-date composite anomaly maps) are plotted in color. Low level wind vectors are colored blue where significant according to similar re-sampling test performed for the u- and v-components separately. Significance is everywhere a function of magnitude and location. The reference period for computing anomalies is 1950 – 1999, as elsewhere. The anomalies are computed from 24-hour averaged fields.

Figure 8. July 23 2006 anomalies of MSLP and wind at 995 sigma level (a), 500m geopotential height (b), and precipitable water (c). Units, contours, arrows and significance are the same as in Figure 7. The color scale has been extended to allow for larger spread of these one-date anomalies, which was also accounted for in the re-sampling significance testing scheme, i.e. noise distribution was re-sampled using 1-day random maps.

Figure 9. Evolution of July 2006 regional DD_{99} (a) and DN_{99} (b) average station magnitude compared to composite evolution of 6 other major daytime and 5 nighttime events from 15 days before to 15 days after the peak magnitude of events. Peaks are dated relative to event type. Average Tmax (red) and Tmin (blue) regional magnitude (circles and thick lines) are displayed in an envelope of total spread of the relevant composite. X's on black line represent 2006 magnitude evolution.

Figure 10. Evolution July 2006 compared to composite evolution of 5 other major daytime and 5 nighttime events from 15 days before to 15 days after the peak magnitude of events. All indices were averaged over rectangles outlined in black over relevant plates on Figures 7 and 8 and anomalies computed relative to JJA climatology. MSLP anomaly gradient (Great Plains box – California Shore box: (a), Z500 averaged over the Washington box (b), PRWTR anomaly averaged over the California/Nevada box or region (125 –115W, 42.5 – 32.5N: (c), low-level (995 sigma) wind convergence: (d) and warming due to low-level temperature advection into the region: (e), and vertical velocity (omega, negative ≡ upwards) at 850hPa over the region: (f). Circles with thick red and blue lines are composite average daytime and nighttime event evolutions. Envelopes are drawn around composite maxima and minima. Black lines punctuated with X's represent evolutions of the 2006 event. For ease of interpretation, smoothing was performed via means of running medians using the 4(3RSR)2H method (Tukey 1977). To

illustrate the mild effect of this smoothing, the raw time series for 2006 is also drawn in the thin black line. A strict comparison requires that the smoothed version (thick black line with X's) be compared to the colored envelopes.

Figure 11. Evolution July 2006 precipitation (thick black line with X's) compared to composite evolution of 5 other major daytime and 5 nighttime events from 15 days before to 15 days after the peak magnitude of events. Precipitation values are daily accumulations (in mm) averaged over all stations. The composite envelopes and *median* precipitation in thick blue and red lines with circles are displayed for nighttime and daytime events, following convention established by Figures 9 and 10. However, no smoothing has been done.

Figure 12. Local overall daytime binned magnitude ($DD^*_{99}{}^{j} = \Sigma_{s^*,d^*}(DD_{99}{}^{j,s,d})$, where s* and d* refer to the particular summer and dates spanned by the event), circle colors correspond to the lowest $DD^*_{99}{}^{j}$ of the bin) accumulated over the duration of each of four selected events *and* rainfall (arrows) accumulated over the period from 1 date prior to 5 dates following the peak date. Blue (green) arrows signify local amounts in excess of summer (average summer month) totals. Overall regional magnitude, aggregated over all stations, for each event is given in Table 4 and Figure 6. Titles for each panel give the year of the event, % of stations with measurable rainfall, total accumulated rainfall, and average accumulated rainfall per wet station.

Figure 13. California and Nevada land area-averaged albedo derived from visible channel satellite data at 10, 12, 14 and 16 hours on each day from -8 before to 8 days after the peak event date. Data for the 2002 event (c), day +1, at 16 hours, was missing.

Figure 14. (a) Linear trend computed at each pixel of the PRWTR averaged for July. Significant trends (95% significance level in a two-tailed test) are colored. (b) July PRWTR in a box [132.5-125W, 25-35N] and linear trend significant well above the 99% level for both the full and base (not shown) periods. (c) Daily evolution anomaly of PRWTR in the same box for 31 days around the peak of great daytime and nighttime heat waves as well as the 2006 event (as in Figure 10c). (d) Daily anomaly of the v-component of the 995 sigma-level wind averaged over the southern margin [125-117.5W, 32.5-27.5N] of the California-Nevada region; and the u-component of the wind averaged over the box [127.5-125W, 30-35N] along the region's southwestern margin, averaged together and representing the northeastward advection from the PRWTR source region delineated on panel (a) into southwestern California.

TABLE CAPTIONS

Table 1. Overview of definitions for heat wave magnitude M. Locally (at station j=1,…,N, N=95), on a particular date (d=1,…,92 or June 1,…, August 31) of a particular summer (s=1948,…,2006), $M_{99}^{j,s,d}$ is exceedance over the local 99th percentile (T_{99}^{j}, computed for the base period of 50 summers, 1950-1999). So, $M_{99}^{j,s,d} = (T_{s,d,j} - T_{99,j})$ if $T_{s,d,j} > T_{99,j}$ or zero otherwise. These local daily values are aggregated over space (all stations j=1,…,N) and time (all summer dates d=1,…,92, or particular event durations: s*, d*) by summation (Σ) performed over the subscripted parameters. Asterisks (*) refer the specific summer and days spanned by a particular event. In the text, we refer to M computed for daytime or maximum temperatures (T=Tmax) as *degree days* (DD), while M computed for nighttime or minimum temperatures (T=Tmim) is referred to as *degree nights* (DN). Regional magnitudes can be computed only using local magnitudes when the percentile threshold temperature is exceeded for at least n consecutive dates, as is done in the text for n=1, 2, and 3 (M[n] = DD[n] or DN[n]). Magnitude is in degrees C.

Table 2. Linear trends in regional magnitude expressed in local degree days and nights (i.e. averaged over all stations) per decade are given for heat waves of local duration of at least 1, 2 and 3 days or nights. Significance levels (*90%, **95%, ***99%) correspond to two-tailed tests for not equaling zero. A test of strictly positive trend would result in systematically higher significance (i.e. 95%, 97.5% and 99.5%, respectively). All trends are positive.

Table 3. Correlation coefficient between, and trends within, the heat wave component indices displayed in Figure 5 for regional daytime (regular font) and nighttime (*italic font*) heat waves. Correlations between daytime and nighttime heat wave components are displayed along the main diagonal (regular bold font). All correlations are significant at the 99% level after adjusting for autocorrelation. Trends are in appropriate units per decade (in local degree days for maximum magnitude, i.e. per average station; % stations for spatial extent; and days for regional duration) are displayed along the bottom row with significance (*90%, **95%, ***99%, under a two-tailed test). For brevity, all results are shown for heat waves of unspecified local duration (n = 1 day or night).

Table 4. Peak dates of the greatest regional heat waves on record listed in order of largest magnitude. Only events listed in **bold** font were **not** used for composite results in Figures 8, 10, 11 and 12. Overall magnitude, defined as $DD^*_{99} = \Sigma_{j,s^*,d^*}(DD_{99}^{j,s,d})$ and $DN^*_{99} = \Sigma_{j,s^*,d^*}(DN_{99}^{j,s,d})$, were asterisk (*) refers to the particular summer and days spanned by the specific event, i.e. the overall magnitude over the entire duration of the event and over all stations associated with each event. DD^*_{99} and DN^*_{99} are given in regular and *italic* font, respectively, as are the peak spatial extent and regional duration. Results are for unspecified local durations (n=1).

FIGURE 1

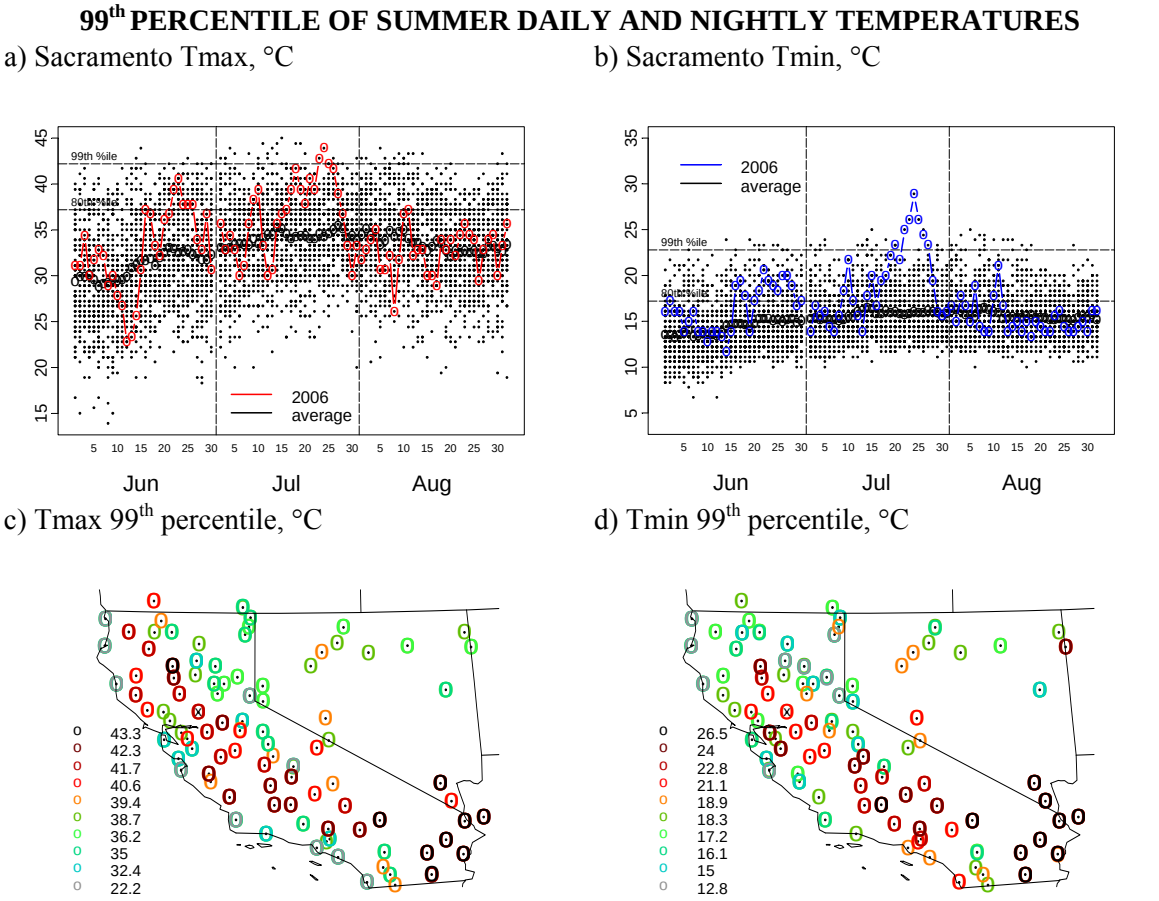

Figure 1. Observed Tmax (a) and Tmin (b) plotted in dots for every date of every summer on record with average (black circles) and 2006 observations (colored circles) for Sacramento (WSO City station). The 99th percentile threshold (dashed line) was computed over the 1950 – 1999 climatology. By definition, daytime or nighttime heat waves occur on days when Tmin or Tmax exceed this threshold over a given minimum duration (n=1,2,3). They are quantified locally as sums of exceedances over the 99th percentile. Panels (c) and (d) depict the approximate (in bins) 99th percentiles of summertime Tmax and Tmin, respectively, at each station. Regional heat waves are quantified as exceedances over the local 99th percentile, *and given a specific minimum duration,* summed over all stations. "X" marks Sacramento.

FIGURE 2

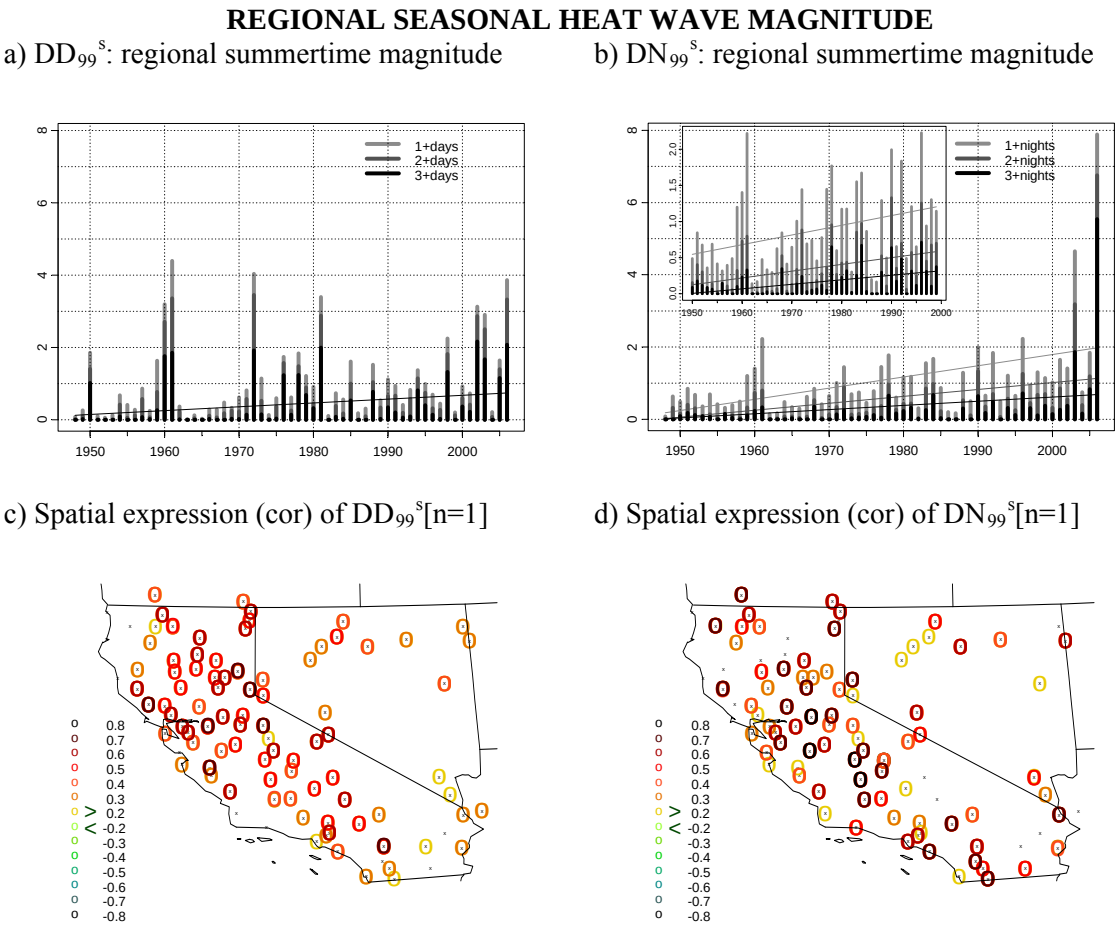

Figure 2. Regional seasonal magnitudes, DD_{99}^{s}[1,2,3] (a) and nights, DN_{99}^{s}[1,2,3] (b) as defined in Table 1. Linear regression lines are shown for the entire record (1948-2006) and over the base period (1950-1999, inset) only where slope is significantly different from zero (two-tailed test) at above the 95% significance level (see Table 2). DD_{99}^{s} and DN_{99}^{s} are correlated at 0.6, 0.54 and 0.47, for local durations of at least n = 1, 2 and 3 consecutive days and nights, respectively. DD_{99}^{s} (DN_{99}^{s}) time series are obviously highly correlated with each other, e.g. above 0.99 and above 0.94 for daytime and nighttime events, respectively, given any combination of local durations. The spatial expressions of the region-wide indices (DD_{99}^{s} and DN_{99}^{s}) given local minimum durations of one day or night (n=1) are shown as correlations with local $DD_{99}^{j,s}$ (c) and $DN_{99}^{j,s}$ (d). Correlations greater than 0.22 are significant with 95% confidence. All colored circles represent significant correlations.

FIGURE 3

a) Daily/nightly regional magnitude (n=1)

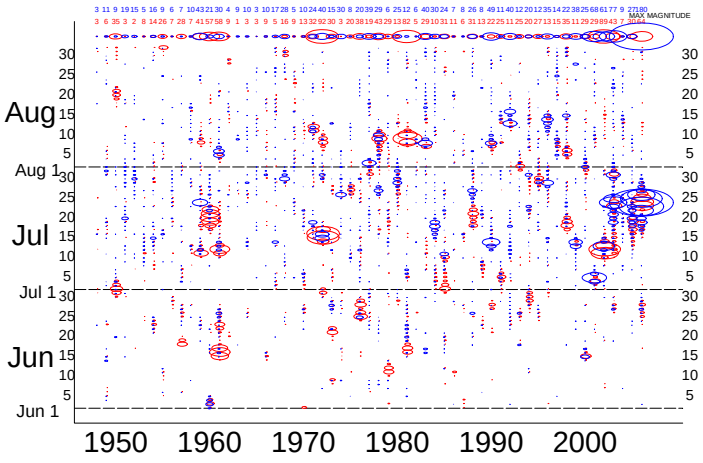

b) Daily/nightly regional magnitude (n=3)

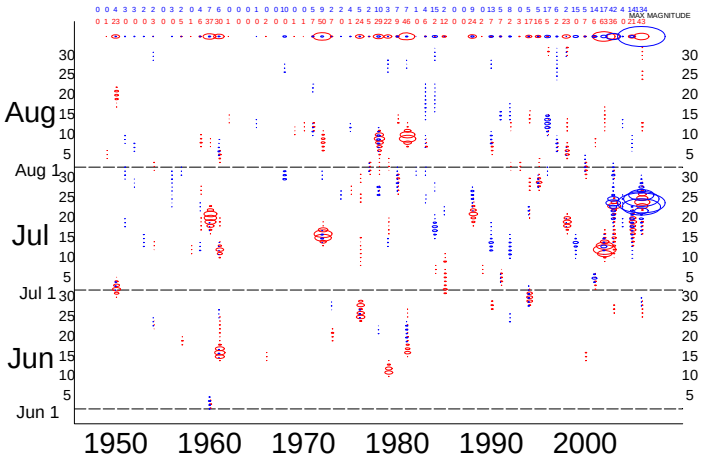

Figure 3. The daily-level magnitude of regional heat wave activity as defined in Table 1: $DD_{99}^{s,d}$ (red ovals) and $DN_{99}^{s,d}$ (blue ovals). The x-axis corresponds to each year on record, while the y-axis corresponds to each summer date. Regional magnitude for unspecified local duration, n=1 (a) and local duration of at least 3 consecutive dates (b). The larger the oval, the greater the magnitude. The scale is given by the maximum magnitude recorded each summer and shown at the top of each plot and again in Figure 5a,b. The overall magnitude for each summer is shown in Figure 2a,b.

FIGURE 4

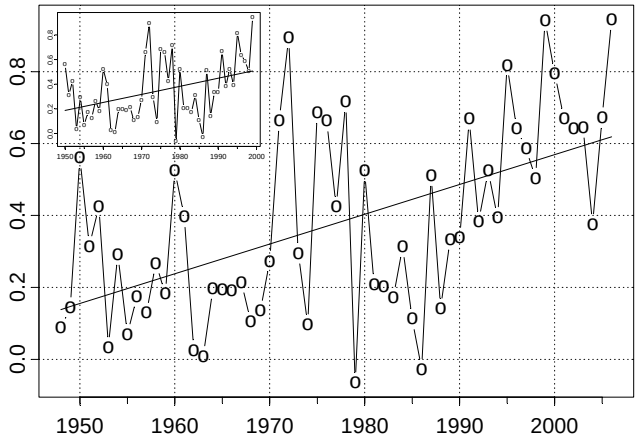

Figure 4. Correlations between each summer's daily and nightly heat wave magnitude (columns of red and blue bubbles on Figure 3a). This reflects the degree to which regional daytime and nighttime heat waves are coincident, regardless of local duration (n=1). Correlations above 0.17 (0.24) are significant at 95% (99%). Linear trends for the entire period as well as for the base period (1950 – 1999, inset) are statistically significant with over 99% confidence (two-tailed test).

FIGURE 5

SEASONAL MAXIMA OF REGIONAL HEAT WAVE COMPONENTS

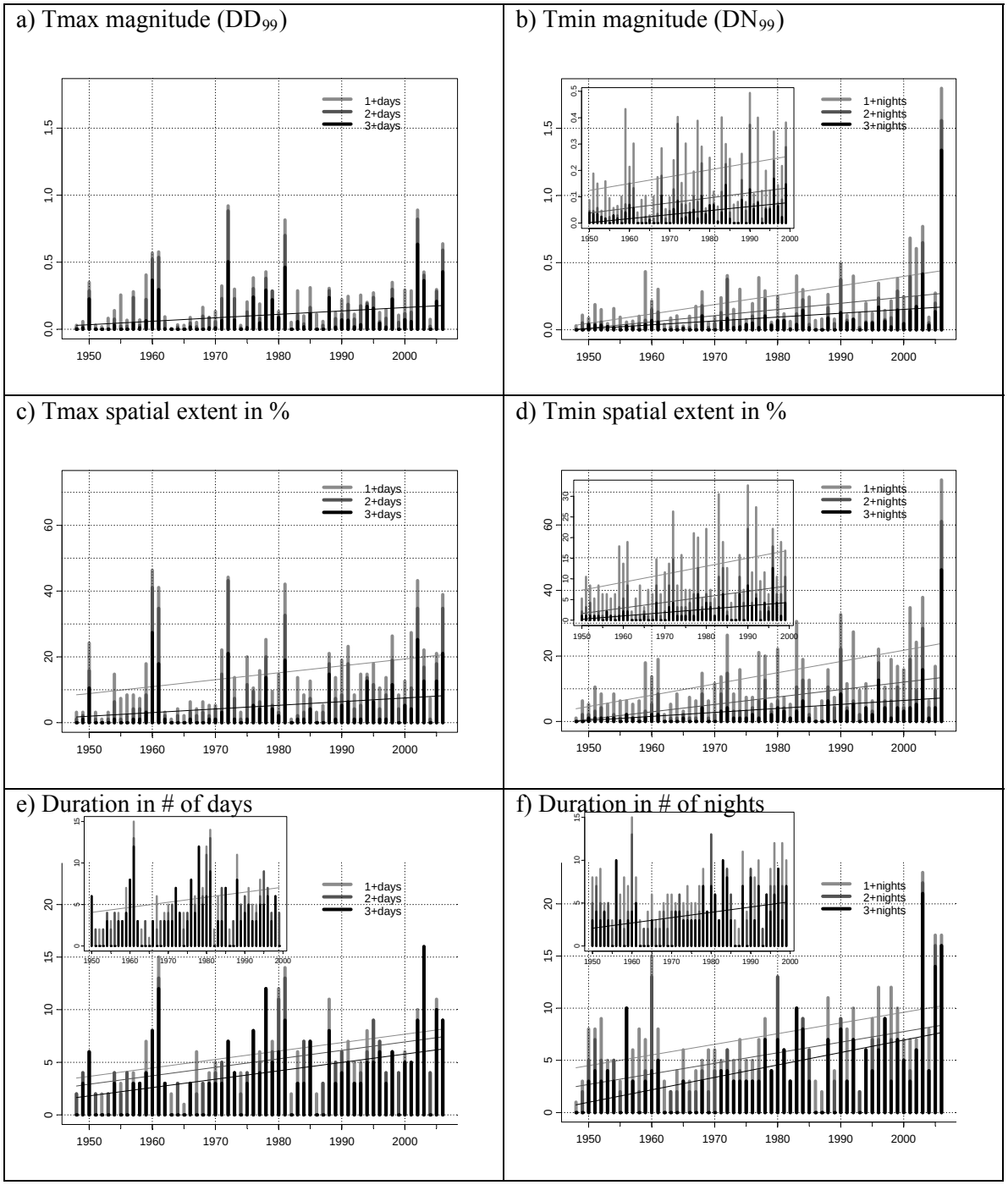

Figure 5. Seasonal maxima of regional heat wave components: total magnitude on the peak day (a) and night (b) of the greatest events, maximum spatial extent in % of stations by day (c) and night (d); and maximum continuous regional duration of daytime (e) and nighttime (f) heat waves. All variables were computed for each summer on record from data presented in Figure 3.

Components were computed given local durations of at least 1, 2 and 3 consecutive days/nights (n=1,2,3) and delineated in progressively darker shades of gray. Correlations between these indices and trends are given in Table 3.

FIGURE 6

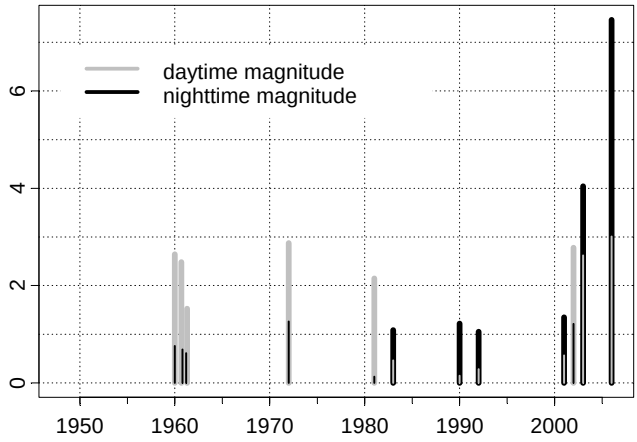

Figure 6. Overall magnitude [cumulative temperature departures (°C) in excess of 99th percentile of each station] of the six daytime (gray) and nighttime (black) great heat waves in California region. Thick (thin) lines delineate the heat wave's primary (secondary) expression, i.e. daytime or nighttime. Magnitude is in degree days/nights per average station, i.e. $DD^*_{99} = \Sigma_{j,s^*,d^*}(DD_{99}{}^{j,s,d})$, where s* refers to the particular summer and d* refers to dates spanned by the event.

FIGURE 7

COMPOSITE ANOMALY MAPS

a) MSLP daytime-type events (mb)

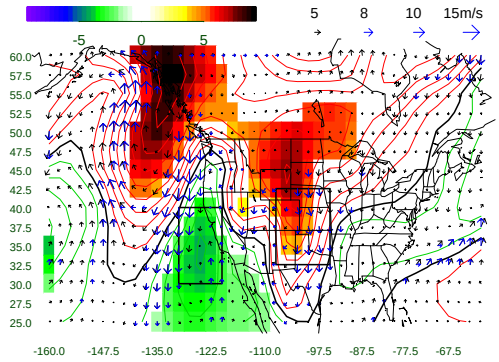

b) MSLP nighttime-type events (mb)

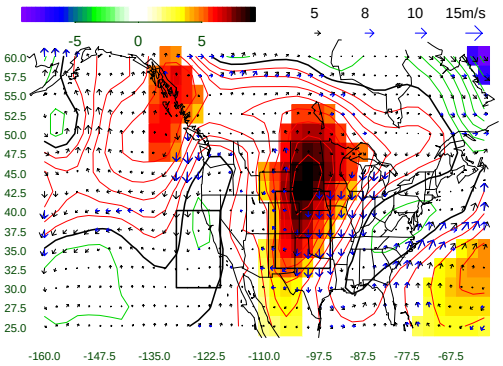

c) Z500 daytime-type events (meters)

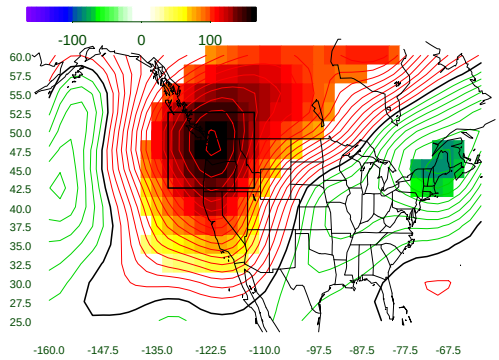

d) Z500 nighttime-type events (meters)

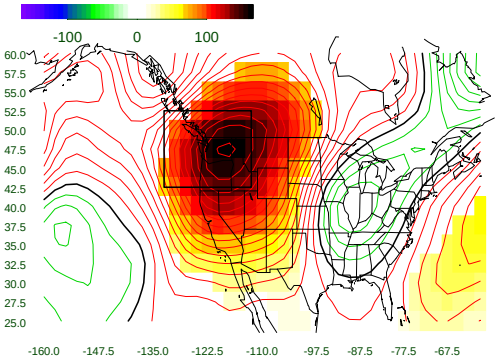

e) PRWTR daytime-type events (kg/m^2)

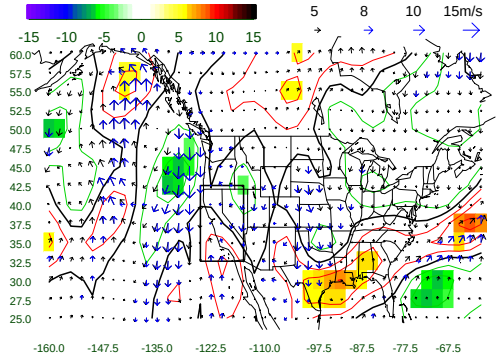

f) PRWTR nighttime-type events (kg/m^2)

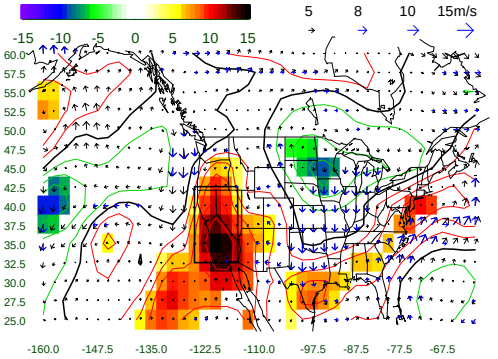

Figure 7. Surface circulation (wind at sigma level 995, arrows in m/s) and mean sea level pressure in millibars (a,b), 500mb geopotential height in meters (c,d), and precipitable water kg/m^2 (e,f) anomalies with respect to JJA mean. Anomalies are composited for the peak days of the largest five daytime events (a,c,e) and the largest five nighttime events (b,d,f) excluding 2006 and 1972 (see Table 4 for exact dates). The data are from the NCEP/NCAR Reanalysis I (Kistler

et al. 2001). Black rectangles outline regions used for evolution plots presented in Figure 10. Contours and colors represent the same anomalies, but only values statistically significant with 95% confidence (two-tailed test) determined via bootstrap re-sampling (performed with 1000 re-sampled 5-date composite anomaly maps) are plotted in color. Low level wind vectors are colored blue where significant according to similar re-sampling test performed for the u- and v-components separately. Significance is everywhere a function of magnitude and location. The reference period for computing anomalies is 1950 – 1999, as elsewhere. The anomalies are computed from 24-hour averaged fields.

FIGURE 8

a) MSLP 2006 (mb)

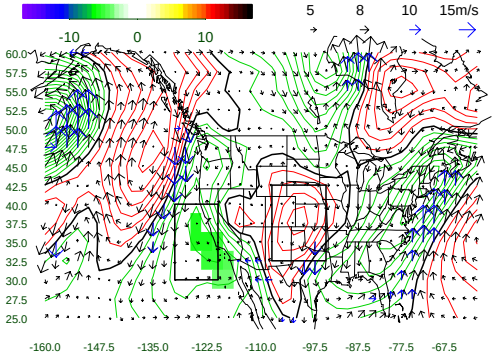

b) Z500 2006 (m)

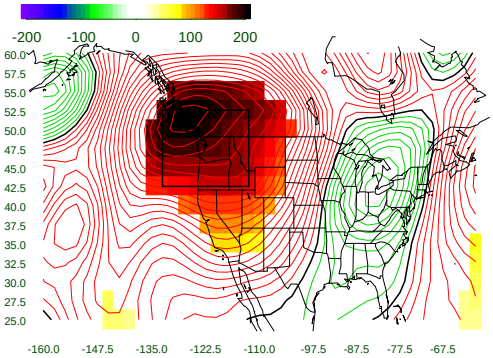

c) PRWTR 2006 (kg/m^2)

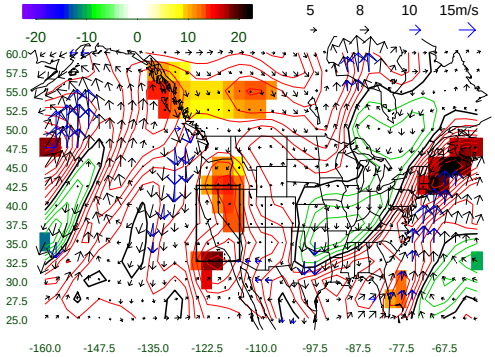

Figure 8. July 23 2006 anomalies of MSLP and wind at 995 sigma level (a), 500m geopotential height (b), and precipitable water (c). Units, contours, arrows and significance are the same as in Figure 7. The color scale has been extended to allow for larger spread of these one-date anomalies, which was also accounted for in the re-sampling significance testing scheme, i.e. noise distribution was re-sampled using 1-day random maps.

FIGURE 9

a) Daytime events: $DD_{99}^{s*,d}$ (Tmax) evolution

b) Nighttime events: $DN_{99}^{s*,d}$ (Tmin) evolution

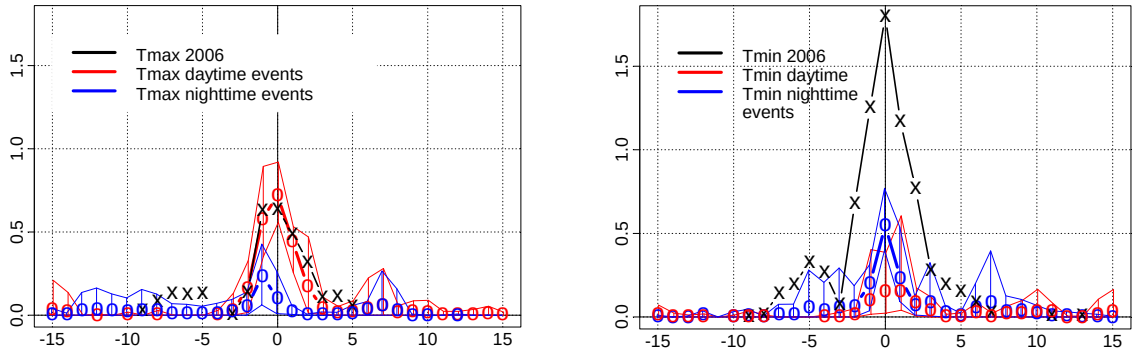

Figure 9. Evolution of July 2006 regional DD_{99} (a) and DN_{99} (b) average station magnitude compared to composite evolution of 6 other major daytime and 5 nighttime events from 15 days before to 15 days after the peak magnitude of events. Peaks are dated relative to event type. Average Tmax (red) and Tmin (blue) regional magnitude (circles and thick lines) are displayed in an envelope of total spread of the relevant composite. X's on black line represent 2006 magnitude evolution.

FIGURE 10

a) MSLP (GP–CA shore), mb

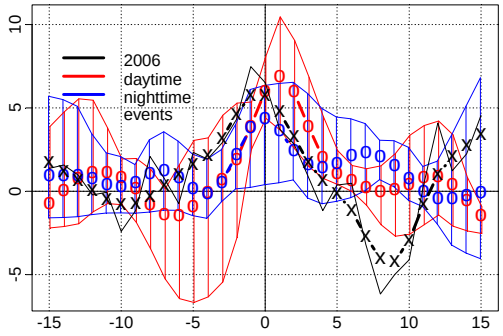

b) Z500 over the northwest, m

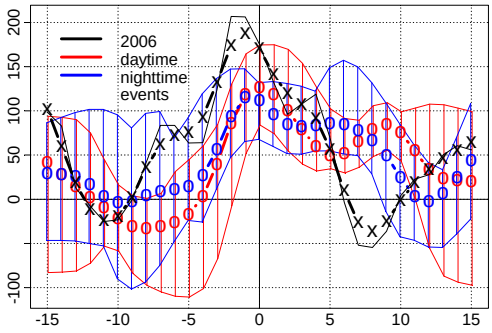

c) PRWTR over CA/NV, mm

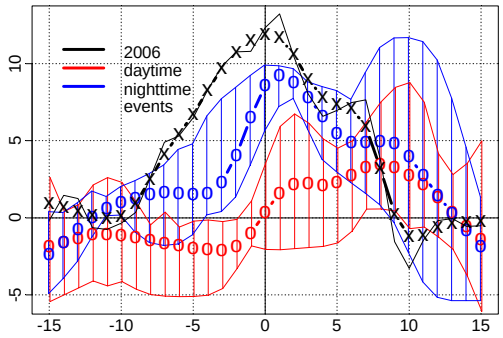

d) Wind convergence, m/s

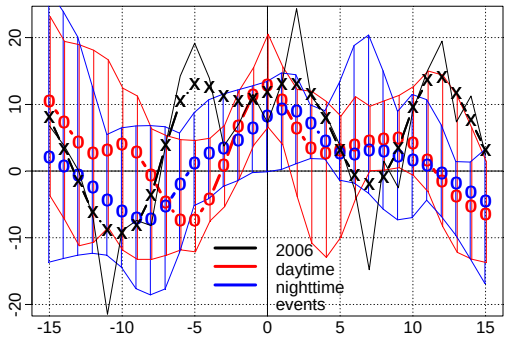

e) Temperature advection, °C/day

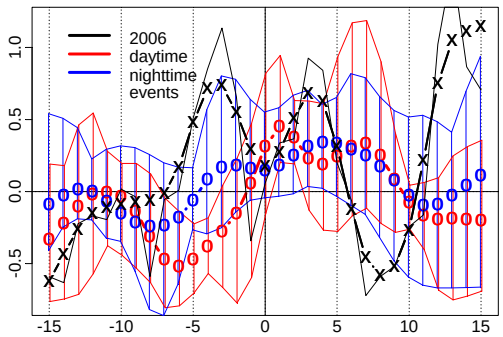

f) Vertical velocity at 850hPa, Pa/s

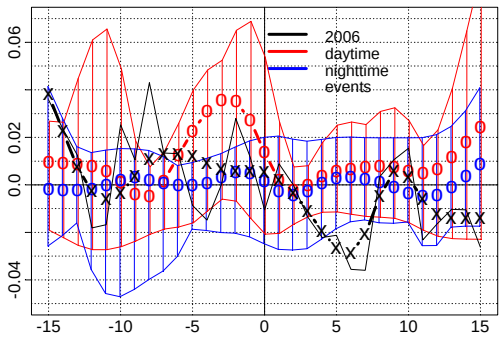

Figure 10. Evolution July 2006 compared to composite evolution of 5 other major daytime and 5 nighttime events from 15 days before to 15 days after the peak magnitude of events. All indices were averaged over rectangles outlined in black over relevant plates on Figures 7 and 8 and anomalies computed relative to JJA climatology. MSLP anomaly gradient (Great Plains box – California Shore box: (a), Z500 averaged over the Washington box (b), PRWTR anomaly averaged over the California/Nevada box or region (125 –115W, 42.5 – 32.5N: (c), low-level (995 sigma) wind convergence: (d) and warming due to low-level temperature advection into the

region: (e), and vertical velocity (omega, negative ≡ upwards) at 850hPa over the region: (f). Circles with thick red and blue lines are composite average daytime and nighttime event evolutions. Envelopes are drawn around composite maxima and minima. Black lines punctuated with X's represent evolutions of the 2006 event. For ease of interpretation, smoothing was performed via means of running medians using the 4(3RSR)2H method (Tukey 1977). To illustrate the mild effect of this smoothing, the raw time series for 2006 is also drawn in the thin black line. A strict comparison requires that the smoothed version (thick black line with X's) be compared to the colored envelopes.

FIGURE 11

Daily Precipitation Totals (mm/station)

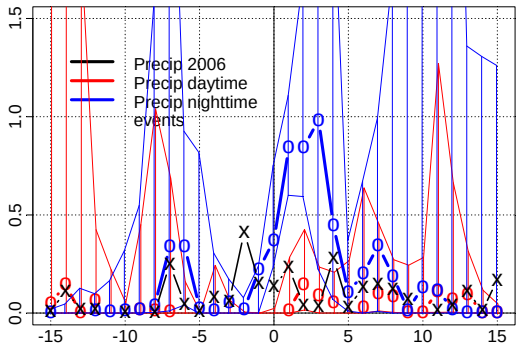

Figure 11. Evolution July 2006 precipitation (thick black line with X's) compared to composite evolution of 5 other major daytime and 5 nighttime events from 15 days before to 15 days after the peak magnitude of events. Precipitation values are daily accumulations (in mm) averaged over all stations. The composite envelopes and *median* precipitation in thick blue and red lines with circles are displayed for nighttime and daytime events, following convention established by Figures 9 and 10. However, no smoothing has been done.

FIGURE 12

a) 2006: 26% wet, 85mm, 3.4mm/stn

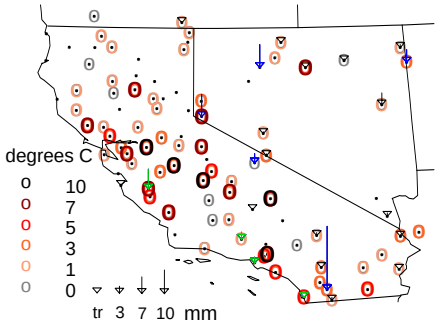

b) 2003: 38% wet, 233mm, 6.5mm/stn

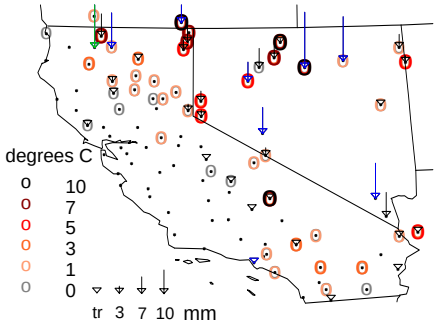

c) 2002: 15% wet, 62mm, 4.5mm/stn

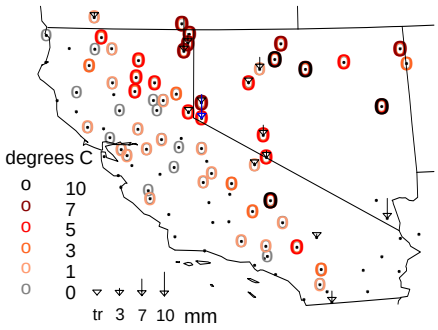

d) 2001: 48% wet, 388mm, 8.4mm/stn

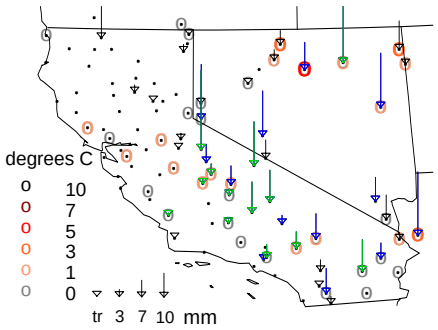

Figure 12. Local overall daytime binned magnitude ($DD^*_{99}{}^{j} = \Sigma_{s^*,d^*}(DD_{99}{}^{j,s,d})$, where s* and d* refer to the particular summer and dates spanned by the event), circle colors correspond to the lowest $DD^*_{99}{}^{j}$ of the bin) accumulated over the duration of each of four selected events *and* rainfall (arrows) accumulated over the period from 1 date prior to 5 dates following the peak date. Blue (green) arrows signify local amounts in excess of summer (average summer month) totals. Overall regional magnitude, aggregated over all stations, for each event is given in Table 4 and Figure 6. Titles for each panel give the year of the event, % of stations with measurable rainfall, total accumulated rainfall, and average accumulated rainfall per wet station.

FIGURE 13

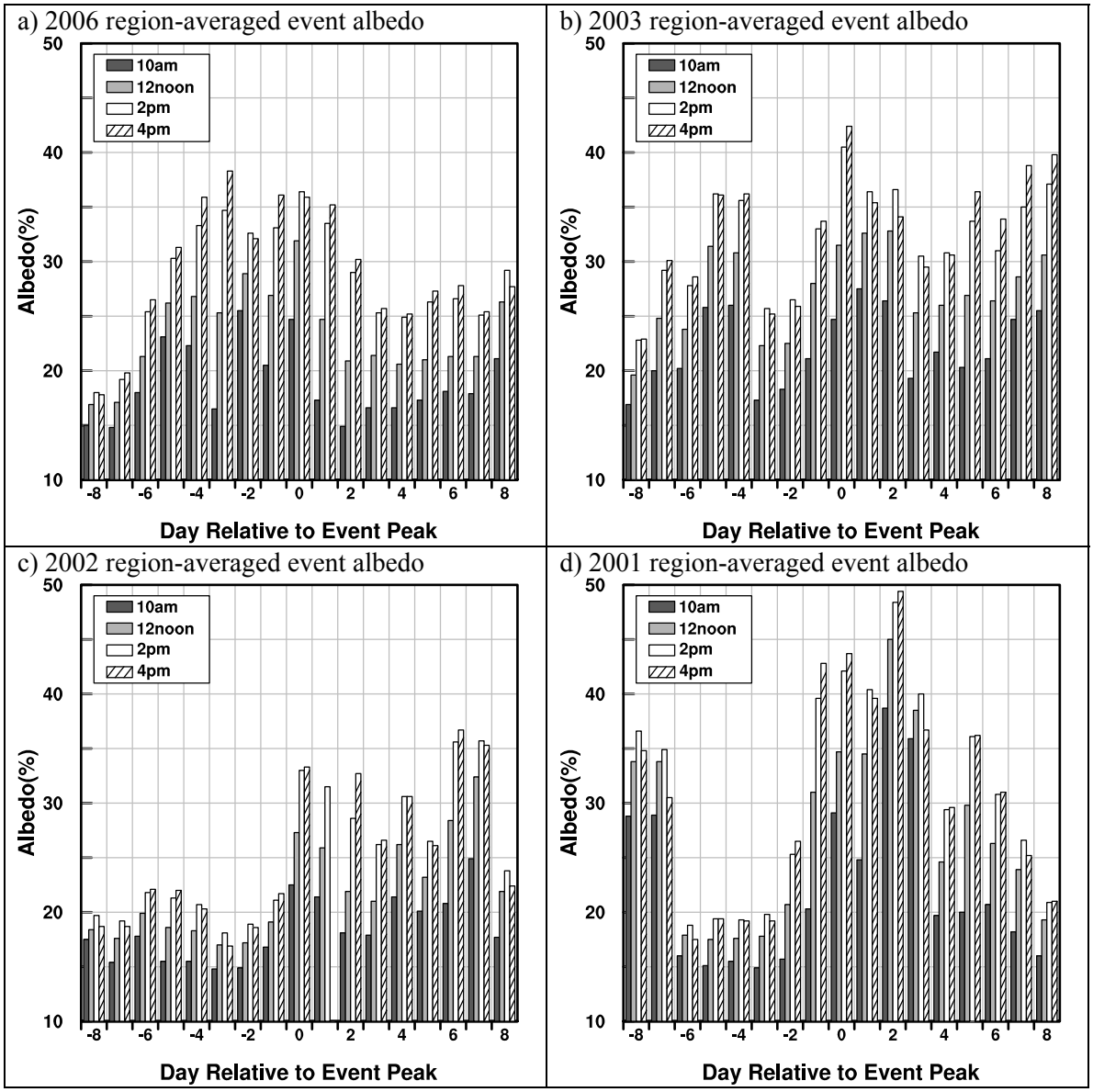

Figure 13. California and Nevada land area-averaged albedo derived from visible channel satellite data at 10, 12, 14 and 16 hours on each day from -8 before to 8 days after the peak event date. Data for the 2002 event (c), day +1, at 16 hours, was missing.

FIGURE 14

a) JJA trend in PRWTR (kg*m^{-2}/decade)

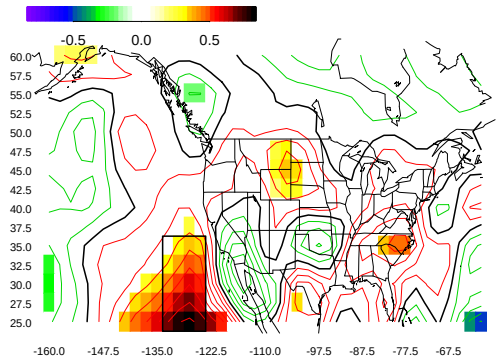

b) July trend in box **132.5-125W, 25-35N**

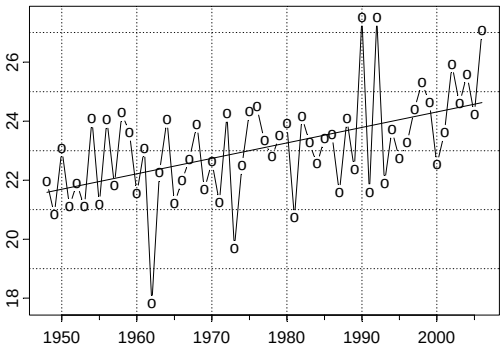

c) PRWTR anomaly in off-shore box (kg/m^2)

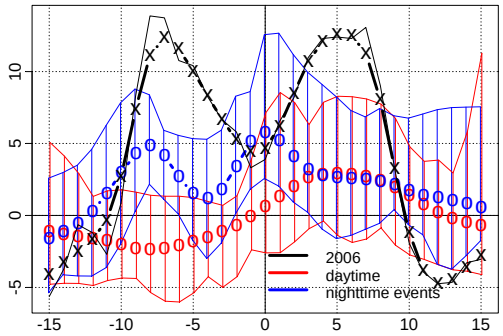

d) Advection into S and S-W California (m/s)

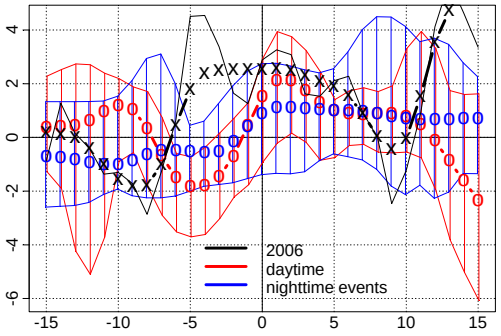

Figure 14. (a) Linear trend computed at each pixel of the PRWTR averaged for July. Significant trends (95% significance level in a two-tailed test) are colored. (b) July PRWTR in a box [132.5-125W, 25-35N] and linear trend significant well above the 99% level for both the full and base (not shown) periods. (c) Daily evolution anomaly of PRWTR in the same box for 31 days around the peak of great daytime and nighttime heat waves as well as the 2006 event (as in Figure 10c). (d) Daily anomaly of the v-component of the 995 sigma-level wind averaged over the southern margin [125-117.5W, 32.5-27.5N] of the California-Nevada region; and the u-component of the wind averaged over the box [127.5-125W, 30-35N] along the region's southwestern margin, averaged together and representing the northeastward advection from the PRWTR source region delineated on panel (a) into southwestern California.

TABLE 1

MAGNITUDE	DAILY	SEASONAL	EVENT
LOCAL	$M_{99}^{j,s,d} = T^{j,s,d} - T_{99}^{j}$	$M_{99}^{j,s} = \Sigma_d(M_{99}^{j,s,d})$	$M^*_{99}{}^{j} = \Sigma_{s*,d*}(M_{99}^{j,s,d})$
REGIONAL	$M_{99}^{s,d} = \Sigma_j(M_{99}^{j,s,d})/N$	$M_{99}^{s} = \Sigma_{j,d}(M_{99}^{j,s,d})/N$	$M^*_{99} = \Sigma_{j,s*,d*}(M_{99}^{j,s,d})/N$

Table 1. Overview of definitions for heat wave magnitude M. Locally (at station j=1,…,N, N=95), on a particular date (d=1,…,92 or June 1,…, August 31) of a particular summer (s=1948,…,2006), $M_{99}^{j,s,d}$ is exceedance over the local 99th percentile (T_{99}^{j}, computed for the base period of 50 summers, 1950-1999). So, $M_{99}^{j,s,d} = (T_{s,d,j} - T_{99,j})$ if $T_{s,d,j} > T_{99,j}$ or zero otherwise. These local daily values are aggregated over space (all stations j=1,…,N) and time (all summer dates d=1,…,92, or particular event durations: s*, d*) by summation (Σ) performed over the subscripted parameters. Asterisks (*) refer the specific summer and days spanned by a particular event. In the text, we refer to M computed for daytime or maximum temperatures (T=Tmax) as *degree days* (DD), while M computed for nighttime or minimum temperatures (T=Tmim) is referred to as *degree nights* (DN). Regional magnitudes can be computed only using local magnitudes when the percentile threshold temperature is exceeded for at least n consecutive dates, as is done in the text for n=1, 2, and 3 (M[n] = DD[n] or DN[n]). Magnitude is in degrees C.

TABLE 2

	DD_{99}[1] : DN_{99}[1]	DD_{99}[2] : DN_{99}[2]	DD_{99}[3] : DN_{99}[3]
TRENDS 1948:2006	**0.15* : *0.31******	**0.14* : *0.24******	**0.11**: *0.17******
TRENDS 1950:1999	**0.03 : *0.13*****	**0.03 : *0.09******	**0.02 : *0.05******

Table 2. Linear trends in regional magnitude expressed in local degree days and nights (i.e. averaged over all stations) per decade are given for heat waves of local duration of at least 1, 2 and 3 days or nights. Significance levels (*90%, **95%, ***99%) correspond to two-tailed tests for not equaling zero. A test of strictly positive trend would result in systematically higher significance (i.e. 95%, 97.5% and 99.5%, respectively). All trends are positive.

TABLE 3

CORRELATION BETWEEN MAXIMAL HEAT WAVE COMPONENTS

Maximal components	**MAGNITUDE**	**SP EXTENT**	**DURATION**
MAGNITUDE	**0.46**	*0.96*	*0.58*
SP EXTENT	0.91	**0.46**	*0.65*
DURATION	0.67	0.70	**0.60**
TRENDS 1948:2006	0.03* : *0.07***	2.1** : *3.4****	0.8*** : *1.0****
TRENDS 1950:1999	0.01 : *0.03***	0.9 : *1.9****	0.6** : *0.4*

Table 3. Correlation coefficient between, and trends within, the heat wave component indices displayed in Figure 5 for regional daytime (regular font) and nighttime (*italic font*) heat waves. Correlations between daytime and nighttime heat wave components are displayed along the main diagonal (regular bold font). All correlations are significant at the 99% level after adjusting for autocorrelation. Trends are in appropriate units per decade (in local degree days for maximum magnitude, i.e. per average station; % stations for spatial extent; and days for regional duration) are displayed along the bottom row with significance (*90%, **95%, ***99%, under a two-tailed test). For brevity, all results are shown for heat waves of unspecified local duration (n = 1 day or night).

TABLE 4

GREAT DAYTIME HEAT WAVES

Peak Date	Overall Magnitude	Peak Sp Extent	Regional Duration
1972, 7, 14	**2.87/*1.26*** **(°C)**	**44/*26*** **(%)**	**7/*6*** **(days)**
2002, 7, 11	2.78/*1.21*	43/*24*	10/*7*
1960, 7, 19	2.64/*0.76*	46/*14*	9/*15*
1961, 6, 15	2.48/*0.68*	41/*12*	15/*8*
1981, 8, 8	2.15/*0.13*	42/*7*	7/*4*
1961, 7, 11	1.53/*0.61*	40/*14*	15/*8*

GREAT *NIGHTTIME* HEAT WAVES

Peak Date	Overall Magnitude	Peak Sp Extent	Regional Duration
2006, 7, 23	***7.46*/3.01** **(°C)**	***74*/39** **(%)**	***17*/9** **(days)**
2003, 7, 23	*4.04*/2.62	*38*/22	*23*/16
2001, 7, 4	*1.35*/0.57	*35*/27	*7*/5
1990, 7, 13	*1.22*/0.15	*33*/19	*9*/6
1983, 8, 7	*1.08*/0.46	31/14	5/3
1992, 8, 12	*1.05*/0.28	*27*/8	*7*/5

Table 4. Peak dates of the greatest regional heat waves on record listed in order of largest magnitude. Only events listed in **bold** font were **not** used for composite results in Figures 8, 10, 11 and 12. Overall magnitude, defined as $DD^*_{99} = \Sigma_{j,s^*,d^*}(DD_{99}{}^{j,s,d})$ and $DN^*_{99} = \Sigma_{j,s^*,d^*}(DN_{99}{}^{j,s,d})$, were asterisk (*) refers to the particular summer and days spanned by the specific event, i.e. the overall magnitude over the entire duration of the event and over all stations associated with each event. DD^*_{99} and DN^*_{99} are given in regular and *italic* font, respectively, as are the peak spatial extent and regional duration. Results are for unspecified local durations (n=1).